SOME RESULTS OF PILOTED SIMULATOR INVESTIGATIONS
ON WINDSHEAR DETECTION SYSTEMS AND ICON DISPLAY CONCEPTS

W.F.J.A. Rouwhorst and H. Haverdings
National Aerospace Laboratory (NLR), Flight Division,
PO Box 90502,
1006 BM Amsterdam

Abstract

In 1993 and 1994, two manned investigations were carried out on the NLR moving base Research Flight Simulator (RFS), concerning several aspects involving the use of an advanced forward-looking windshear detection system in the final approach phase of a flight.

In the first (1993) experiment, three windshear detection systems were evaluated separately, or in combination, together with three specific flight procedures, without presenting any weather (or windshear) information to the crew on a weather type of display. The three systems evaluated consisted of functional models of: a reactive windshear detection system, a non-scanning LIght Detection And Ranging (LIDAR) forward-looking windshear detection system, and a ground-based Terminal Doppler Weather Radar (TDWR) system. With the latter a ground-to-air data-uplink connection to the aircraft cockpit was simulated.

To assess the safety aspects involved, a safety risk model was developed. The model and experiences gained with it will be described. Furthermore, final results and conclusions of the 1993 piloted experiment are presented.

In the second (1994) experiment described, a reactive and a scanning forward-looking LIDAR system were evaluated. The latter produced coloured windshear icon information on an EFIS/NAV display, using two different concepts. The flight procedure evaluated, was coupled to a systems integrated threat-level based windshear alerting concept. Pending a full data analysis, only some preliminary results and conclusions of this second experiment are given.

Abbreviations and Acronyms

AGL   Above Ground Level
AT   Auto throttle
AWO   All Weather Operations
CDU   Central Display Unit
CRT   Cathode Ray Tubes
DB   Downburst
DLR   Deutsche Forschungsanstalt für Luft- und Raumfahrt e.V., Germany
EFIS   Electronic Flight Instrument System
EICAS   Engine Indicating and Crew Alerting System
FAS   Final Approach Speed or Flight deck Alerting System

FD   Flight Director
FH   Flight Hazard
FHF   Flight Hazard Factor
GARTEUR   Group for Aeronautical Research and Technology in Europe
GPWS   Ground Proximity Warning System
ILS   Instrument Landing System
JAR   Joint Airworthiness Regulations
LIDAR   LIght Detection And Ranging
LLJ   Low-Level Jet
KLM   The Royal Dutch Airlines
KNMI   The Royal Netherlands Meteorological Institute
MAC   Mean Aerodynamic Cord
MCCP   Manual Crew Coordination Procedures
MERS   Mental Effort Rating Scale
NAV   NAVigation (display)
NIVR   Netherlands Agency for Aerospace Programs
NLR   National Aerospace Laboratory, the Netherlands
NM   Nautical Miles
ONERA   Office National d'Etudes et de Recherches Aérospatiales, France
PF   Pilot Flying
PFD   Primary Flight Display
PNF   Pilot Not Flying
POD   Probability Of Detection
RFS   Research Flight Simulator
RLD   Netherlands Department of Civil Aviation
TDP   Touch Down Point
TDWR   Terminal Doppler Weather Radar
WTA   Windshear Training Aid

Notations not explained in the main text

A_x, A_z body specific forces
$\vec{e}_{laser}$ unit vector aligned with laser beam
h_{RA} Radio altitude
V, V_{GS} Groundspeed
V_{FAS} Final Approach Speed
V_{ref} Reference speed
V_{TAS} True airspeed
W_x longitudinal wind component; tailwind positive
W_z vertical wind component; downdraught positive
α, α_{stall} (stall) angle of attack

Rouwhorst & Haverdings

Introduction

Windshear, defined as a deterministic change in wind velocity and/or wind direction, remains a concern in aircraft safety. There's no guarantee that aircraft performance will be sufficient to cope with the energy loss resulting from a windshear. Its danger should not be underestimated, as numerous accident and incidents have shown and the best advice is to avoid it.

Early 1996, the first forward-looking windshear detection systems have become commercially available to the airline community[1],[2],[3]. Enhanced (or upgraded) Doppler weather radar systems like AlliedSignal/Bendix-King's RDR-4B, Rockwell/Collins' WXR-700X and the new MODAR 3000 radar of Westinghouse will enter the market. The market entry of these new products concludes a period of activities aimed at reducing the accident and/or incident rate related to windshear. This period started with the introduction of the Windshear Training Aid (WTA) Program in 1987[4], and led in 1990 to a mandate of the FAA (see FAR § 121.358[5]) which demanded certain types of aircraft to have a windshear detection system installed before 31st December 1993. However, some operators e.g. North West, American Airlines and Continental Airlines, were granted an extension to 31 December 1995 (under exemption 5256), to acquire technical and operational experience with the new types of forward-looking windshear detection systems that were still under development at that moment. Technical issues such as ground clutter suppression and reliable detection of so-called "dry" windshear (e.g. windshear with very low radar reflectivity characteristics) had to be overcome. The fact that these systems have now received full type certification [6],[7],[8], proves that these problems have been solved satisfactory in the eyes of the regulation authorities. However, apart from a reliable detection of the dangerous weather phenomenon, also issues such as integration within the Flight deck Alerting System (FAS)[9] and the establishment of proper flight operations (procedures) had to be faced. Despite the fact that the Industry-proposed and implemented solution(s) have been accepted by the regulation authorities, these latter issues still need attention and further improvement.

In 1993 and 1994, The National Aerospace Laboratory NLR performed two piloted simulator trials regarding issues described above and will perform a third evaluation in mid 1996. The major part of these activities were performed under contracts of the Netherlands Agency for Aerospace Programs (NIVR) and the Netherlands Department of Civil Aviation (RLD).

ICAS paper 7-1.3[10] already presented a full description and some initial results of the 1993 experiment. This paper presents the final results of the first simulator experiment and will repeat some important aspects of the experimental set-up for sake of completeness. Furthermore it will address the second (1994) experiment but only preliminary results are presented, as final results are pending a full data analysis.

The Research Flight Simulator (RFS)

Both experiments were carried out on the moving-base Research Flight Simulator (RFS) of NLR. This simulator consists of a side-by-side cockpit mounted on a four-degrees-of-freedom motion system (pitch, roll, yaw and heave), see Fig.1. The full-glass cockpit has a total of six cathode ray tubes (CRTs) and two central display units (CDUs) comparable with a level of sophistication of the Boeing 747-400 cockpit, see Fig.2. Outside view is generated by a model-board television system with images collimated at infinity.

Models used

Aircraft model

A fully non-linear model of a four-engined, heavy weight transport aircraft was simulated. The model includes delay in engine spool-up time responses, and effect of flap and gear setting on aerodynamic performance. The aircraft equations of motions were updated at 20 Hz. Aircraft parameters used in the experiment were based on the maximum landing weight configuration of 285800 kg, with a centre of gravity at 25% MAC.

Windshear models

The windshear models that have been developed and were used during the experiments were a downburst (or microburst) model[10], a low-level jet model[11] and another "neutral" shear model. To account for the atmospheric boundary layer effect, the windshear models were mixed with a boundary layer model. Due to real-time restrictions in the calculation process of the pulsed forward-looking windshear detection system, a three dimensional spatial grid in the area of the runway was developed on which the wind data generated by the above models were stored. Above a certain reference height the grid data was integrated with pre-stored tabled wind data. This table data only contained horizontal wind profiles as a function of height. All windshear models produced stationary (Earth-fixed) wind fields.

In the 1993 experiment, three versions of each windshear model were used. The "neutral" shear model for example produced either a light headwind change, a light crosswind change or a severe crosswind change.

In the 1994 experiment, the windshear could, if detected by the forward-looking sensor, be visually observed on the EFIS/NAV display. In order to prevent the crew from recognizing the windshear many more windshear versions were used. These were categorized in classes of severity (not extreme/just extreme/extreme) and threat

Rouwhorst & Haverdings

position (threat/ no threat) with respect to relative distance between centre of the shear cell and the runway centre line.

Turbulence model

To investigate the effect of turbulence on overall crew and system performance, the NLR Non-Gaussian turbulence model[14] was used and enhanced. The model features intermittency, patchiness, influences of altitude and windspeed on scale length and intensity, and "above/below clouds" effects. To account for the anisotropical interplay (effect) between windshear and turbulence, the suggestion by Woodfield and Woods[15] was followed to add a fraction of the absolute value of the vertical wind component into the various turbulence intensities. The general expression for the rms intensity of the turbulence velocities was defined as:

$$\vec{\sigma}_{u_g, v_g, w_g} \equiv \begin{Bmatrix} \sigma_{u_g} \\ \sigma_{v_g} \\ \sigma_{w_g} \end{Bmatrix} = \begin{Bmatrix} c\sqrt{u_w^2+v_w^2} + d|w_w| \\ c\sqrt{u_w^2+v_w^2} + d|w_w| \\ c\sqrt{u_w^2+v_w^2} + d|w_w| \end{Bmatrix} \quad (1)$$

where u_w, v_w and w_w are wind components. The parameter values c and d were varied as function of the desired turbulence intensity level:

c=0 , d=0 'no' turbulence
c=0.1 , d=0.03 'light-to-moderate' turbulence
c=0.13 , d=0.07 'moderate-to-severe' turbulence

Windshear detection system models

Reactive system

The reactive windshear detection system model developed has been based on information from a simple Sundstrand system[16]. The reactive system is engaged automatically below 1500 ft AGL. The reactive system alert logic in the first experiment was based on an F-factor calculation in aircraft wind axes, with the F-factor defined as:

$$F = \frac{-A_x*\cos(\alpha) - A_z*\sin(\alpha) + \dot{V}_{TAS}}{g}*L_1 + \frac{\dot{h}_{RA}}{V_{TAS}}*L_2 \quad (2)$$

where L_1 and L_2 are height-dependent scale factors to reduce nuisance effects at low altitude. This is a systems equivalent of the well known equation for F[17]:

$$F = \frac{1}{g}\frac{dW_x}{dt} + \frac{W_z}{V_{TAS}} \quad (3)$$

The instantaneous F-factor of Eq.(2) was used to calculate the averaged F-factor F_{av} (averaged in time), which is defined in the Technical Standard Order (TSO-117)[18] as:

$$F_{av}(t) = \frac{1}{T_x}\int_{t-T_x}^{t} F(\tau)\,d\tau \quad (4)$$

with T_x being the filter time window. If the calculated averaged F-factor exceeded some specified limits a "CAUTION" or a "WARNING" alert was generated in the cockpit and remained present for at least three seconds. A "CAUTION" would be given in case of a performance *increasing* situation. A "WARNING" alert was given when the aircraft encountered a severe performance *loss*. It is noted that in the 1994 experiment not Eq.(2) but Eq.(3) was used in the averaging process.

Forward-looking windshear detector

As forward-looking sensor a functional model of a CO_2 lidar (laser) was developed. The laser beam could be stabilized in three ways, viz. a) fixed in the airframe, b) pitch-stabilized, and c) flight path angle-stabilized. The mode of laser beam stabilization was an experimental variable. During the 1993 experiment no scanning mode was provided, i.e. the beam was aligned within the longitudinal plane. To calculate the windshear hazard from the laser the laser F-factor derived by Bowles[17] was used:

$$F_{laser} = \frac{V}{g}\frac{d}{dx}(V_{Doppler}) + \frac{W_z}{V_{TAS}} \quad (5)$$

In its mechanisation the vertical wind component (W_z) was deleted and not estimated by other means. The Doppler speed $V_{Doppler}$ includes horizontal as well as vertical wind components, and was calculated from the dot product

$$V_{Doppler} = \vec{e}_{laser}\cdot(\vec{V}_I - \vec{W}) \quad (6)$$

where $\vec{V}_I$ is the inertial speed vector, and where $\vec{W}$ is the windspeed vector. The F-factor for the laser also is averaged in a manner similar to F_{av}, by taking an equivalent spatial integration along the laser beam, as follows:

$$F_{laser_{av}}(r) = \frac{1}{R_x}\int_{r-R_x}^{r} F_{laser}(x)\,dx \quad (7)$$

The distance variable r runs from a minimum range value R_{min}, determined by system parameters, to a

Rouwhorst & Haverdings

1831

maximum range R_{max}, where the maximum range is limited by precipitation and/or the presence of the ground. The distance R_x and filter time T_x are related by:

$$R_x = V.T_x \qquad (8)$$

Three levels of filter time T_x, or distance R_x, were used in the 1993 experiment.

In the 1994 experiment the laser was enhanced with a scanning mode such that it could generate in real time the necessary information to present windshear icons on an EFIS/NAV display. These icons would both present the position, threat and area coverage of the windshear. Multiple icons could be present, indicating more than one cell. Icons were all of a circular form and were connected to an alert logic.

TDWR system

For the ground-based detection system a functional model of the Terminal Doppler Weather Radar (TDWR) was developed. Because of real-time problems with the simulator software this functional model could not be implemented in time, and hence the effect of this sensor on the alert was used instead. Therefore the time when the warning would occur was varied randomly. Three "levels" were foreseen, viz. 'early', 'timely' and 'late'. These values, or labels, were associated with an altitude range, based on range from touchdown, where the TDWR alert occurred with a uniform probability of occurrence within the altitude interval, see Table 1.

Table 1 TDWR probability of detection (POD)

TDWR POD	height range (ft)	distance from touchdown (nm)
'early'	1000 - 2000	3.14 - 6.28
'timely'	500 - 1000	1.57 - 3.14
'late'	0 - 500	0 - 1.57

Ground Proximity Warning System (GPWS) model

A reactive windshear detection system model will in general be incorporated within a ground proximity warning system (GPWS). To enhance operational realism a GPWS model has been defined, based on general information of SUNDSTRAND's Mark VII GPWS[16] including six modes out of the existing seven modes. The seventh mode, a windshear detection, annunciation and alerting mode, was replaced by an in-house-defined

mode which regulated the priority between the six modes of the GPWS, the reactive windshear system alerting and the forward-looking windshear detection system alerting possibilities.

Alerting aspects

Windshear alerting and other aural alerts

Both visual and aural alerts were generated in accordance with the requirements of the FAA[18],[19], and were provided to the crew. Visual windshear alerts depend upon the type of windshear sensor detecting the windshear, and consisted of either a label "WINDSHEAR" or "WINDSHEAR AHEAD" presented on the lower c.q. upper part of an EFIS/PFD, or both labels simultaneously.

The labels were generated both for "caution" or "warning" alerts. Cautions were presented in amber colour, while warnings were presented in red colour, both for the airborne reactive and forward-looking windshear detection system.

A master caution/warning button/light in front of the pilot flying, located near the top of the instrument panel, was also illuminated if an airborne windshear alert occurred. The light could be reset by pressing the button.

Aural windshear alerts were given by a computerized voice through the cockpit speakers calling out the words "WINDSHEAR" in case of an alert from the reactive system, or the words "WINDSHEAR AHEAD" in case of a forward-looking system alert. It was given in three subsequent cycles for warnings, but in only one cycle in case of a caution. If windshear alerts were generated by the simulated TDWR system a warning sound (chime) would trigger the pilot's attention and a data-link message was presented on the lower EICAS panel. Three different formats, with increasing information content, were used, viz.

Format A: "TDWR alert"
Format B: "TDWR alert"
      "Position ..nm from threshold".
Format C: "TDWR alert"
      "Position ..nm from threshold"
      "Max wind change ..kts"

Other aural cues to the crew consisted of engine sounds, protection warnings (like stick shaker, outer and middle marker beacon sounds, and call-outs belonging to the six modes of operation of the GPWS.

Aural alerting priority

An aural priority schedule was defined and implemented which gave overall priority to the windshear alerts.

Rouwhorst & Haverdings

In order of highest priority the sequence of aural alerts was given by:
1) Reactive windshear system alert above forward-looking windshear alert
2) Highest windshear alert (threat) level
3) GPWS Modes 1 through 6
4) Other (system) alerts, e.g. TDWR data-uplink alerts

1993 Experiment

Experimental factors

In view of the objectives the following number of experimental variables were defined:
a) flight procedure (1="safety first", 2="cautious", 3="daring"). See explanation below.
b) type of windshear detection sensor (No sensor, reactive system, forward-looking laser, TDWR, or the combination of an airborne with the TDWR sensor);
c) type of windshear (neutral, low-level jet, downburst)
d) turbulence level (no, moderate, severe)
e) critical F-factor level F_{crit} (-0.08, -.10, -0.15).
f) allowed speed change ΔV for the critical F-factor (10, 20, 25 kts).[10]
g) type of laser beam stabilization (body pitch, along speed vector, inertial pitch).
h) precipitation (0 mm/hr, 15 mm/hr, 50 mm/hr), or equivalently a maximum effective range of the laser of 8000 m, 3300 m or 1500 m.
i) TDWR probability of detection POD ('Early', 'Timely', 'Late', see Table 1).
j) the TDWR data uplink format. (Format A,B or C)

Table 2 Experiment trials versus sensor configuration

Trial No.	Sensor
1	no sensor (baseline config.)
2	reactive system
3	laser system
4	TDWR system
5	sensor mix

Conduct of the 1993 experiment

Three crews participated in the experiment. Of each crew, both members acted as Pilot Flying (PF). The total experiment was subdivided per crew into two sets of 5 trials each, distributed over two days. The trials were devoted to a single sensor or set of windshear sensors, with the no sensor cases as the experiment baseline, see Table 2. Furthermore, each crew was given two out of three procedures to follow, as it would be too difficult for the crews to be trained for three different types of flight procedures.

Procedures

Approach procedure

In both experiments only approaches were studied. Each approach was initiated at a distance of 13 nm (24 km) from the runway threshold, 2 nm (3704 m) left of the extended centre line of the runway at an intercept heading of 30 deg of the final approach course at an altitude of 2000 ft (610 m). The aircraft was stabilized and trimmed for a horizontal flight condition with an indicated airspeed of 205 kts, flaps set at 10 degrees and landing gear retracted. The pilots were instructed to perform Cat.I approaches (with a Decision Height of 200 ft) and to execute a normal landing approach, according to normal operational practice and normal safety standards, thereby applying the Manual Crew Coordination Procedures (MCCP). The Final Approach Speed (FAS) used, was 156 kts (Vref + 5 kts).
The pilot not flying (PNF) performed the ATC communication and assisted the PF in his flying task, according to the MCCP. The crew had to fly the approaches manually, but use of the autothrottles was allowed. Furthermore the crew was assisted in ILS-tracking by a flight-director (FD). This FD, however, was not designed to give windshear guidance commands in the experiment of 1993. Because of this, the FD had to be disregarded if a go-around was initiated in case of a windshear situation.

Go-around procedures

The crew was given two options as to the type of go-around to perform, viz. the standard, normal go-around (normally involving configuration changes), or the Windshear Training Aid (WTA) go-around (no change of configuration). This latter type had to be adhered to whenever there was a reactive system windshear alert, or when the crew felt they were actually in a windshear. In other cases they were left free to choose which procedure they would follow.

Flight procedures evaluated

Three flight procedures were tested. They consisted of applying some speed increment(s) and to initiate a go-around, in case of one or more windshear warnings, depending upon altitude, see Table 3.

Rouwhorst & Haverdings

Table 3 Speed increments and flight procedures

| type of warning | speed increment | | flight proc. |
	above 500'	below 500'	
single	GA	GA	safety first
	15	20	cautious
	15	20	daring
double/ multiple	GA	GA	safety first
	20	GA	cautious
	20	20	daring

The following flight procedures were tested:

1) safety first: a go-around had to be made at any time there was a RED alert (i.e. a WARNING).

2) cautious penetration: When there was a first RED alert from any windshear sensor during the approach above 500 ft, the flight speed had to be increased to $V_{ref}+15$ kts, or immediately to $V_{ref}+20$ kts when below 500 ft, and the approach continued. If a second RED alert (from any warning system) was generated above 500 ft then the speed had to be increased further to $V_{ref}+20$ kts. For any (remaining) second RED alert below 500 ft, a go-around had to be made.

3) daring penetration: the flight speed had to be increased to $V_{ref}+15$ kts when there was any RED alert above 500 ft. If a first RED alert occurred below 500 ft, speed also had to be set to $V_{ref}+20$ kts. If a second RED alert (from any other warning system) was generated either above or below 500 ft, then speed had to be increased to $V_{ref}+20$ kts. This procedure tended to drive the crew towards continuing the approach at a fairly high speed, rather than abort and make a go-around.

Data collection

Pilot subjective data

After each run the crew had to fill out a questionnaire.
Both the pilot flying and the pilot not flying had to answer questions related to situational awareness. The pilot flying furthermore had to answer questions related to piloting effort to maintain speed, track the ILS, etc., and also had to rate his (mental) workload using a subjective (ordinal) (mental) effort rating scale (MERS).[21]. After the experiment a debriefing questionnaire had to be filled in and a discussion was held.

Measured data

Sixty four parameters were recorded at a frequency of 20 hz and stored on magnetic tape. Afterwards statistical parameters such as the mean, the root mean squares (rms), the standard deviation, the mean deviation and minimum and maximum values were calculated for 3 defined segments:

- segment 1 (Upper ILS): ILS altitude between 1500 and 500 ft, or moment of making a go-around;
- segment 2 (Lower ILS): ILS altitudes between 500 and 50 ft, or moment of making a go-around;
- segment 3 (Go-around segment): from the moment of go-around initiated until the moment of altitude capture.

Due to the long runway length available, landing distance would not create an operational problem. The landing segment (4) defined, consisted of touchdown criteria only. To this purposes data was recorded at certain specific events. The most important were:

- passage of the 1500', 1000', 500', 250', 100' and 50' ft altitudes (based on distance-to-go to runway touchdown point);
- the moment of touchdown;
- the moment the go-around button was depressed;
- the moment a windshear sensor alert was generated.

Data analysis

The data obtained in the experiment were analyzed in several ways. For instance an ANOVA (= ANalysis Of VAriance) was applied on all statistical segment measures, pilot questionnaire data and on data of some events. Furthermore, parametric and non-parametric tests, e.g. the F-test c.q. the Kruskal-Wallis test, were performed where appropriate.
Concerning the statistical analysis, the following levels of statistical significance (p) were defined:

- weakly significant: $p < 0.10$
- significant: $p < 0.05$
- highly significant: $p < 0.01$

Safety assessment

In order to be able to evaluate the effect of windshear sensors, type of windshear and flight procedures tested, on the safety of operation, a number of variables were analyzed. Furthermore, two different methods were used for analysis purposes:
- a factor analysis
- a probability analysis (Bayesian approach)
Both methods will be explained below.

Safety investigation using Factor analysis

The question of flight safety is a hard one to answer. In order to obtain some measure of flight safety in a

Rouwhorst & Haverdings

windshear environment, the following list of 11 variables was assumed to play a role in flight safety:

1. pilot perceived windshear hazard (subjective measure)
2. maximum angle of attack, or stall margin (relative to stall angle of attack) per flight
3,4 minimum and maximum pitch angle during the flight
5. minimum airspeed per flight
6. minimum inertial speed during flight
7. minimum (i.e. worst) F-factor of the flight.
8. minimum (i.e. worst) F_{av}-factor during flight
9,10 minimum and maximum vertical acceleration during the flight
11. minimum energy height margin (difference between actual and a reference value)

Note that for each variable only one value was obtained per measurement run (total flight), i.e. over all segments involved.

Several of the variables were correlated, i.e. if one varied, so did the other. The information contained within the correlation matrix was used by factor analysis to determine which independent factors, or groups of variables, were "hidden" within the set of variables given. When applying factor analysis to the variables given above, it turned out that only one independent factor was needed to describe the various effects. This factor has subsequently been named 'Flight Hazard' (FH). The factor loadings upon the variables included were determined. In case of normalization, these loadings also are the correlation coefficients between the factor and the variables. From inspecting these loadings it became clear that perceived windshear hazard, maximum minus minimum pitch angle (i.e. the peak-to-peak pitch change), minimum stall margin, minimum airspeed, minimum F_{av} and the peak-to-peak vertical acceleration change were the greatest contributors to FH. The smallest absolute loading was on minimum energy height margin.

So the above given 11 variables could be replaced by a single factor (FH), which is one of the advantages of applying factor analysis. The 'flight hazard' was further transformed into the 'Flight Hazard Factor' by using the minimum and maximum value of FH, and scaling between zero and one. When denoting flight hazard factor by 'FHF', then the following formula was applied:

$$FHF = \frac{FH - FH_{min}}{FH_{max} - FH_{min}} \qquad (9)$$

Some results with the 'FHF' will be given.

Rouwhorst & Haverdings

Safety analysis using the Bayesian approach

The following general probability rules apply for a Bayesian approach:

$$P(X \cup Y) = P(X) + P(Y) - P(X \cap Y) \qquad (10)(a)$$

with

$$P(X \cap Y) = P(X|Y).P(Y) \qquad (10)(b)$$

Here $P(X \cup Y)$ is the probability on the union of event X or Y, $P(X \cap Y)$ is the probability on the intersection of both events and $P(X|Y)$ is the conditional probability of event X, given that event Y has occurred. If there is no dependence in probability between event X and Y, then $P(X|Y) = P(X)$. In that case $P(X \cap Y)$ becomes $P(X).P(Y)$.

The question of safety has been subdivided into *flight* safety and *landing* safety. Concerning the flight runs made in this experiment, the following definition of the probability of an unsafe event is given:

$$P(A) = \text{Probability of event A} \qquad (11)$$

where the following events are defined:

A = unsafe events during the run
A_{FL} = unsafe events during the flight portion of the run
A_{LD} = unsafe events during the landing portion of the run
GA = event of making a go-around during the run; the adjoint event is $\overline{GA}$.

Per definition one has the following relationship:

$$P(GA) + P(\overline{GA}) = 1 \qquad (12)$$

Using the probability theory the total probability of an unsafe event during each run can be stated as:

$$P(A) = P(A \cap \overline{GA} \cup A \cap GA)$$
$$= P(A \cap \overline{GA}) + P(A \cap GA) \qquad (13)$$
$$= P(A|\overline{GA}).P(\overline{GA}) + P(A|GA).P(GA)$$

The statement above means in fact:
the probability of an unsafe event during a run is equal to the probability of an accident during the run, given that no go-around has occurred,
OR
the probability of an unsafe event during a run, given that a go-around has been made.

In case of a go-around, the probability of an unsafe event during the run, is made up of the flight portion only. In case of a landing (no go-around) both the flight and landing portion are included. This implies that the conditional probabilities in Eq.(13) can be rewritten.

I) for the approaches resulting in a go-around it is found that:

$$P(A|GA) = P(A_{FL}|GA) \qquad (14)(a)$$

while
II) for the approaches ending in a (safe) landing:

$$P(A|\overline{GA}) = P(A_{LD}) + P(A_{FL}|\overline{GA}) \qquad (14)(b)$$

Note that Eq.(14b) describes the sum of the flight part and the landing part. Substituting the above two equations into Eq.(13) yields the total run probability:

$$P(A) = P(A_{LD}).P(\overline{GA}) + P(A_{FL}) \qquad (15)$$

where obviously we have that $P(A_{LD})$ is the landing safety risk and $P(A_{FL})$ is the flight safety risk. The latter is given by:

$$P(A_{FL}) \equiv P(A_{FL}|GA).P(GA) + P(A_{FL}|\overline{GA}).P(\overline{GA}) \qquad (16)$$

Eq.(16) shows that flight safety includes both the safety considerations during the approach part of the flight as well as the go-around part. Landing safety in Eq.(15) is only related to the safety at moment of touchdown, although normally also the safety during the roll-out after landing should be included.

The probability $P(\overline{GA})$ was calculated *per category* of interest, e.g. for the safety-first flight procedure flying on a downburst, etc. The conditional probabilities were calculated *per run* using the mean and standard deviation of those variables which were involved in the risk of an unsafe event, together with the normal probability distribution of these variables. It was assumed that on the respective segments the variables of interest were normally distributed, with a mean and standard deviation as determined per segment per run. Data inspection revealed that this assumption was not too severely violated.

Numerical limits were defined in order to calculate the probability of an unsafe event.

Numerical limits for flight safety analysis

It was hypothesized that the following variables, conditions, etc. were important concerning the risk of an unsafe event during the flight part of a run:

1) angle of attack $\alpha \leq \alpha_{stall}$. This relates to the risk of stalling the aircraft, which is defined as a crashworthy condition. In this paper the angle-of-attack *margin* is taken, i.e. $\alpha_{margin} = \alpha_{stall} - \alpha$;

2) height above terrain **h**. Obviously this relates to the risk of hitting the ground. Because of the generally large trend (i.e. monotonic increase) in this variable, the standard deviation became quite large, and therefore use of the standard deviation became unsuitable for probability calculations. Therefore height was <u>not</u> used for the go-around segment flight probability calculations and negative glideslope deviations were used instead for the non go-around cases;

3) airspeed $Va > Va_{max}$. Whenever the airspeed exceeds a maximum, there is a risk of parts flying off the aircraft or damage due to aerodynamic overload. For the aircraft type used this speed has been set 10 kt above the flap 30 limit speed of 180 kts, 231 kts with flaps 20 (go-around condition), and 238 kts for flaps 10 degrees;

4) vertical acceleration A_z. Whenever the vertical acceleration exceeds a maximum (or minimum) there is a risk of structural damage. Extreme values set in the report are +2.5 g and -1 g (flaps up), and +2.5 g and -0.5 g with flaps extended;

5) negative glideslope deviation $\Delta\epsilon_{G.P.}$. This condition was used instead of the height above terrain for the approach phase of the flight. Maximum negative ILS glideslope deviation is set at -2 dots, for the approach phase only, for the go-around segment this parameter was not used.

Numerical limits for landing safety analysis

According to JAR/AWO[20], the following variables contribute to landing safety:

* the longitudinal and lateral coordinates x_{TD} and y_{TD} relative to the touchdown point. When certain values are exceeded then the aircraft is likely to land left or right of the runway ($|y_{TD}| > y_{TDlimit}$), or land too long ($x_{TD} > x_{TDmax}$), with the risk of runway overrun, or land too short ($x_{TD} < x_{TDmin}$), with the risk of landing before the runway;

* pitch angle at touchdown θ_{TD}. When $\theta_{TD} > +11°$ then a tail strike occurs. If $\theta_{TD} < 0°$ then a different limit applies for the sink rate as the aircraft will then be landing on its nosewheel first;

* sinkrate at touchdown $w_{e\ TD}$. When the sinkrate at touchdown is too high then there is a risk of failure of the landing gear, depending on the pitch angle at touchdown. With a negative pitch angle at touchdown the landing will be made on the nosewheel first, and in that case a lower sink rate limit applies;

Rouwhorst & Haverdings

* groundspeed at touchdown V_{GS}. When the groundspeed is too high there is a risk of tire failure, or else runway overrun or wheel brake overheating;
* angle-of-attack α_{TD} at touchdown. This provides the margin to stall angle. Too low a value indicates the risk of a hard landing;
* bank angle at touchdown φ_{TD}. When the bank angle exceeds a certain limit value there is the risk of engine pod strike (for the aircraft type used), with consequent damage and the risk of fire;
* lateral velocity or sideslip angle for structural limit loads. Since the aircraft flown may be landed with lateral forces on the landing gear (due to crabbed landings) this criterion has not been incorporated.

After some iterations the following limit values were set and used in calculating $P(A_{LD})$ in Eq.(15):
* -1000 ft $< x_{TD} < +3800$ ft
* $|y_{TD}| < 21$ m
* $\theta_{TD} < 11^0$ to prevent a tail strike when landing.
* sinkrate $w_e < 1000$ ft/min (5.08 m/s) if $\theta_{TD} \geq 0^0$; and $w_e < 600$ ft/min if $\theta_{TD} < 0^0$ (i.e. for a nosewheel landing)
* $V_{GS} < 203$ kts (max. tire speed)
* $\alpha_{margin} > 0^0$
* $|\varphi_{TD}| < 8.5^0$. This value was taken from a geometrical drawing to provide engine pod clearance with the ground when banking the aircraft

More details about the probability calculation process and limit values per segment are given in Appendix A.

Final results of the 1993 experiment

Basic facts
A total of 180 experimental runs (approaches) were flown, an average of one third through downbursts, but no crashes occurred. A distribution of the number of landings and go arounds of all the experimental runs over crews and flight procedures is given in Table 4.
As can be observed, 127 landings were made against 53 go-arounds (70.6% versus 29.4%). The number of landings increased from about 14% (26 cases) for the 'safety first' flight procedure (procedure 1) to about 30% for flight procedure 3. This is a trend that could be expected since the 3rd ('daring') flight procedure allowed the crews to continue the approach the farthest. However, both landings and go-arounds should be reviewed on their safety, as will be shown later.

Distribution of go-arounds
Fig.3 and Fig.4 present histograms of the distribution of the number of go-arounds (and landings) over flight procedure, windshear type and windshear sensor type.

Table 4 Distribution of number of landings and go arounds over crews and flight procedures

Crew	Flight Procedure							
	1		2		3		Totals	
	L	G	L	G	L	G	L	G
1	11	19	27	3	-	-	38	22
2	15	15	-	-	25	5	40	20
3	-	-	20	10	29	1	49	11
Totals	26	34	47	13	54	6	127	53

Note: L=Landing; G=Go-around

If compared between the types of windshear, Fig.3 shows that most of the go-arounds were made for the downburst (DB) cases, as expected. For the 3rd ('daring') flight procedure, no go-arounds were made in case of a low-level jet (LLJ) or a neutral (N) type of shear, but only if a downburst was encountered. Fig.4 shows that no landings were made with either the reactive system or the laser (lidar) in case of a downburst and the safety first flight procedure.

Fig.5 presents the go-around distribution as function of the altitude segments along the glideslope. There were 4 cases (7,5%) above 1500 ft AGL, but these cases were found to be due to an incorrect execution of the flight procedure evaluated. Furthermore, 94,3% (or 50 cases) was initiated before 100 ft AGL (with even 77,4%, or 41 cases, before decision height of 200 ft AGL) and still 5,7% (3 cases) below 50 feet AGL. A peak amount of 20 (37,7%) go-arounds was initiated between 1000 and 500 ft AGL. This result can be explained from Fig.6, where the average go-around position before the runway touchdown point (TDP) is presented as function of the flight procedure applied. Clearly, go-arounds with the 'safety first' flight procedure were initiated (on average) the farthest from the runway TDP, or equivalently at the higher altitudes, while with the 'daring' flight procedure go-arounds were executed nearest to the runway TDP. In the latter case (with 20 kts speed increment), it was more often possible to overcome the windshear and to continue the approach. If a go-around was initiated, it was generally the result of a destabilized final approach and not of the windshear alerts, hence it was of the standard type.

Rouwhorst & Haverdings

Type of go-around

Since the pilots had an option (in case of a forward-looking windshear alert) to apply either the WTA or the Standard go-around manoeuvre, it was tried to identify if from a statistical point of view there was a pilot preference to either one of these procedures. However, statistical significance of main effects was difficult to determine, due to the fact that go-arounds were not made under all combinations of sensors, windshear types and flight procedures tested.

Fig.7 presents the average distance to runway TDP for both types of go-around. On average the standard type of go-around was made at lower altitudes than the WTA type of go-around. When analyzing the types of go-around for dependency of the flight procedures involved, then Fig.8 shows a statistically highly significant result ($p=0.0087$) if the non-parametric Kruskal-Wallis test is applied. It shows that with the 'safety' first flight procedure, the pilots adhered more to the WTA type of go-around than with the 'daring' flight procedure. With this latter flight procedure most of the go-arounds were of the standard type. However, only six go-arounds were made with the 'daring' flight procedure (see Table 4).

For the 'cautious' flight procedure the division over both types of go-around was almost equal.

Apart from the flight procedure, also the various sensor types involved turned out to be a statistically significant factor for the type of go-around executed. Unexpectedly, Fig.9 shows that the WTA procedure was applied more often with the laser sensor onboard the aircraft, with TDWR or with sensor mix alerts, than with the reactive (or no) sensor configuration. The reason, in case of a reactive sensor, why not all go-arounds were of the WTA type (as briefed) must be found in the fact that sometimes go-arounds were made, after having passed a shear, due to destabilized approach on (very) short final. The results presented above can be further explained from the pilot comments. Those revealed that pilots preferred to adhere to one type of windshear go-around procedure (irrespective of the sensor alert or flight procedure evaluated), as they regarded windshear as a once-in-a-lifetime experience. Therefore they mostly stuck to the WTA type of go-around procedure if initiated after any windshear alert given and allowed by the flight procedure. So, even in the case of the forward-looking sensor alerts, when there generally was more lead time before the shear would be entered, the WTA was executed. However, the lack of windshear situational awareness (no weather and/or windshear information was presented other than the wind vector on the EFIS/NAV display) is expected to be a factor that has contributed to this result, because pilots did not know how long it would take before they would actually enter the shear.

Safety calculation aspects

As some cases resulted in a go-around instead of a landing, the comparison base for safety has to be the *total* safety risk calculated both for the group of cases that led to a landing or to a go-around. For the go-around cases the calculated total safety risk was split up into a risk calculated for the flight part until moment of go-around initiation and a go-around part. For the landing cases the total safety risk was composed of the sum of the flight safety risk (flight part) and the landing safety risk (touchdown safety risk).

Risk drivers

Figures 10 to 13 present the main contributors to the *flight* and *landing* safety risk calculations along the various segments defined. Remarkably, a very significant risk driver was found in the probability of exceeding the flap limit speeds, as represented by Va_{max}, in all flight segments, but especially in the go-around segment. Other drivers were the risk to exceed the -2 dot glideslope deviation (as expected), and the risk to encounter too negative g-loads (Az_{min}). Furthermore the angle of attack margin (α_{margin}) was of relatively higher importance during the go-around than during the other segments. Landing safety was mainly determined by the risk to land short of the runway touchdown point (x_{TDmin}) and the risk to exceed a bank angle of -8 degrees (ϕ_{min}), i.e. left wing down. The risk to exceed +8 degrees (ϕ_{max}) differed from ϕ_{min} due to the fact that low-level crosswinds mostly came from one direction in the experiment.

Flight safety

Statistically, the flight safety differed significantly with the type of windshear and the flight procedure applied, while the type of windshear sensor had no significant effect.

Fig.14a shows both the calculated flight safety risk and the Flight Hazard Factor, i.e. $P(A_{FL})$ and FHF, as a function of the windshear type, for the landing approaches only. Flying in severe windshear (downburst) circumstances clearly formed the highest risk. Note that the FHF, although on a different scale, follows exactly the same trend as $P(A_{FL})$.

The values for the go-around approaches are presented in Fig.14b. Neutral shears and low-level jets formed an equal flight safety risk for the aircraft, although the FHF indicated a difference between both. However, the subjective measure (pilot perceived hazard) within the FHF is expected to be the reason for this as no other reason could be found.

Although the effect is statistically not significant ($p=0.1780$), it can be seen from Fig.15 that the highest flight safety risk was encountered with the mix of

Rouwhorst & Haverdings

sensors, while the highest FHF occurred in the no sensor case. The difference between both risk indicators could not be explained. However, supported by both indicators it can be seen that the safety was best (=lowest flight safety risk or FHF value) with a forward looking windshear detection system (laser) on board of the aircraft.

If grouped as function of flight procedure, Fig.16a-b show that for landing and go-around approaches, the 'daring' (most windshear penetrating) flight procedure had the highest risk. For the landing approaches, the 'cautious' flight procedure had the lowest flight safety risk. The FHF indicates the same trend. For the go-around cases, the 'safety first' flight procedure was found to be the safest. The reason why the trend of the FHF deviates from the flight safety risk figure is again found to be in the pilot perceived hazard during the execution of a go-around. With the 'cautious' flight procedure, very often the core of a downburst had to be crossed, leading to occasionally a severe stall condition with a high altitude loss. Consequently, pilots rated the windshear hazard during these flights much higher than if no stall occurred. With the 'daring' flight procedure a lot of the windshear effect could already be overcome by the extra speed increments allowed and no severe altitude drops or stall situations occurred thus leading to lower hazard ratings.

Go-around safety

Fig.17 compares for the downburst cases only (irrespective of the flight procedure), the flight safety risk for the go-around and the landing cases. As can be observed, both safety indicators follow the same, statistically very significant (p=0.0000), trend:

Safety during go-around approaches was less if compared with continuing the approach. Again, it is noted that for the go-around cases, flight safety risk 'P(A_{FL})' is equal to the total safety risk. however, for the landing cases presented, the landing safety risk 'P(A_{LD})' is not included, so that in this figure we only compare safety on the flight segments!

In the following the FHF will not be presented any more, as the pilot perceived hazard rating was a rating given for the total run and not for the approach, go-around or landing segment separately. The FHF seems a useful tool for safety assessment investigations, but it needs some refinement. Especially, it should include pilot hazard ratings per flight segment in order to better correlate with the safety risk parameters calculated.

Landing safety

Statistically, the following parameters were very significant for differences in the landing safety risk P(A_{LD}): the type of windshear, the flight procedure, the type of windshear sensors and the crews themselves.

Unexpectedly, the landing safety risk was the highest for the low-level jet cases, as can be seen from Fig.18. This result can be explained from the fact that, at moment of touchdown, large bank angles occurred more often in case of low-level jets than with the other shear types.

From Fig.19 it can be concluded that the landing risk for the 'cautious' flight procedure was significantly lower than for the other flight procedures. However, crews only flew two out of three flight procedures. As landing generally is a very complex and demanding task, especially in a simulator, it was no surprise therefore that crews turned out to be a factor in the landing safety risk calculated. Figure 20 shows the results. Trends are not totally consistent especially for the 'daring' flight procedure. It was found that crew 3 generally landed (on average) 200 m longer on the runway than the other two crews, thereby increasing landing risk. It is possible that crew 3 over-compensated altitude, as they were rated on a Boeing 737 type of aircraft and not for a heavy-weight type of aircraft with a correspondingly larger size, as the other two crews were.

Fig.21 presents the finding that any type of windshear sensor, or a mix of sensors, improved landing safety, if compared to the no sensor case. In the latter case, there would be no windshear alert given to increase the speed, so landings were generally made with (on average 2 kts) lesser groundspeed and only after having safely passed the shears. It is suspected that landing the aircraft with a slightly higher speed decreased control difficulty for the crews and made the effect of crosswinds less severe (less decrab and bank angle), thereby improving landing safety. Fig.21 also shows that the best safety improvement occurred for the reactive sensor, while the TDWR gave the smallest improvement. The way the TDWR functionality was modelled and implemented in the experiment is expected to be the reason for this latter result: in contradiction to the other sensor alerts, TDWR alerts were not generated via a realistic windshear sensing process, but via a random generation of different warning times as function of aircraft position.

Total safety
Influence of experimental factors

If analyzed over all cases (landings and go-arounds), the total safety risk, 'P(A)' in Eq.15, was statistically significantly effected by windshear type and crews only. As can be observed in Fig.22, the highest risk occurred for the downburst cases, as expected. Unfortunately, crews turned out to be a statistically significant factor as well, F(3,104)=8.66, p<0.00035. Fig.23 shows the nesting of crews within flight procedure. For the 'cautious' flight procedure the differences between crew 1 and crew 3 were highly significant (p<0.000002). It is possible that this difference was due to differences in

Rouwhorst & Haverdings

learning effects, as this flight procedure was the second one executed by the first crew, but it was the first procedure for the third crew. Also lack of experience in flying heavier types of aircraft may be a reason for this, as explained before.

The type of windshear sensor turned out to have no significant main effect. However, the group consisting of the reactive and the laser sensor had a significantly lower total risk than the group consisting of the no sensor, the TDWR and the mix of sensors, see Fig.24.

Total safety risk of landings and go-arounds

The crews have the choice to either continue and land the aircraft, or to perform a go-around. Therefore total safety risk should be compared between these two situations, see Fig.25 for some results. As can be observed, apart form the 'safety first' flight procedure, the total safety risk in the go-arounds is always higher than for the landing cases. This will be explained later on. Note that in contradiction to the landing cases, the factor "flight procedure" is statistically not significant ($p < .1220$) for the go-around cases. However, the trend shown indicates an increased risk if the flight procedures allows to fly further into the shear with an increased speed.

The total risk for the landing cases was found to be the lowest for the 'cautious' flight procedure, while the risk between the other two flight procedures hardly differed from each other.

If all landing cases are compared against all go-around cases, then Fig.26 shows that the total risk of performing a go-around was much higher than to continue the approach (with a higher speed) and land the aircraft. This result was found extraordinary, difficult to understand and to explain. Therefore, a risk model sensitivity analysis was performed. It was found that the result was totally due to the high probability of exceeding the maximum flap operation speeds during the go-around segment. If this risk element was excluded from the risk model the result would look like Fig.27. This raises the question if the risk of exceeding this maximum flap operation speed(s) is really a serious danger to aircraft safety or not. Perhaps this parameter should not be judged equally severe as the other risk drivers and therefore a different weighting may be appropriate, when compared with the other risk drivers. Additional study is required to answer this question.

Finally, as mentioned before, crews executed more frequently the Standard than the WTA type of go-around. When comparing the total safety risk of these two go-around types, the F-test showed, with $F(1,14)=0.50$ $p < .4899$, that the WTA had a risk value of 0.0464, almost 1.38 times lower (i.e. better) than the standard type of go-around. The risk value for the WTA type even dropped to 0.00368 and the ratio increased to

about 7.38, for $F(1,14)=1.63$ $p < .2226$, when the weighting on the maximum flap operation speed was set to zero. However, as indicated, the results are statistically non-significant.

Some conclusions of the 1993 experiment

The Bayesian risk model developed, although still to be improved, was found very suitable and usefull for the intended risk assessment purposes.

In terms of flight safety the laser sensor consistently had about a five times better (i.e. lower) risk, compared to the (no sensor) baseline case. There was no consistent improvement in flight safety found, when adding a reactive sensor to the aircraft. However, landing safety and total safety were best with either the reactive or the laser sensor. No significant difference was found between these two types of sensors. Total safety risk was significantly higher for the approaches resulting in a go-around than for those resulting in a landing, although this result mainly depended on the risk to exceed the maximum flap operation speeds. If this factor is excluded from the risk model, it was safer to go-around than to continue the approach and land. For the two types of go-arounds that occurred (WTA or standard) no statistically significant difference in total safety risk could be found.

Best overall flight procedure in terms of landing and total safety risk, pilot workload[10] and reduction in go-around rate turned out to be the 'cautious' windshear penetrating flight procedure.

Recommendations from the 1993 experiment

Although the 'cautious' flight procedure came out best, it should be studied more deeply. Furthermore, the effect of adding a windshear display in the cockpit, to improve weather and situational awareness, should be investigated. Crews suggested to modify or improve the *sensor-based* alerting concept into a kind of *sensor integrated threat-level* alerting concept, as too many confusing alerts flooded the cockpit in the multiple sensor configurations evaluated. Also the position of the alerts labels on the EFIS/PFD should be reversed: reactive system labels on top and forward-looking system alerts labels on the bottom. In the future, pilots preferred to be assisted by a flight-director with a state-of-the-art windshear guidance mode, and if possible, based on integrated reactive and forward-looking windshear hazard (sensor) information.

Finally, the risk model should be improved. First of all by including a proper ground collision risk contribution for the go-around phase. Secondly a proper weighting of the risk to exceed the maximum flap operation speeds should be established.

Rouwhorst & Haverdings

1994 Experiment

Experiment description

The 1994 experiment was conducted by GARTEUR (= Group for Aeronautical Research and Technology in EURope) Flight Mechanics Action Group FM(AG07), consisting of ONERA (France), DLR (Germany) and NLR (The Netherlands). The European context was further emphasized by the participation of six crews of the nations involved. Per crew member a total of 27 runs, of which 7 were familiarisation runs, were executed. So in total 240 measurement runs were obtained.

The experiment was split up into two parts. In the first sub-experiment a reactive and a forward-looking windshear detection system were tested separately. Besides, the effect of adding a flight-director with a windshear guidance during a windshear escape was tested. In this sub-experiment no windshear information was visually presented in the cockpit, other than the wind vector on the EFIS/NAV display.

In the second sub-experiment, the effect of presenting windshear *icon* information on the EFIS/NAV-display was investigated. These icons were derived from the information obtained from a real-time scanning laser model.

Threat-level based aural windshear alerts

As a lesson learned from the 1993 experiment, a sensor integrated, *threat-level based* aural alerting concept was defined and evaluated. This implied that aural alerts would only be passed on after the threat-level detected increased to a new level. As no proper information was available during the experiment definition phase, a self-defined threat-level system was used in order to be able to integrate the aural alerting system, the alert labels presented on the EFIS/PFD and the windshear icon information presented on the map mode of the EFIS/NAV-display. The following hazard levels, from lowest to highest priority, were defined:

Hazard level 0 = No hazard
Hazard level 1 = Advisory alert
Hazard level 2 = Caution alert
Hazard level 3 = Caution (suppressed Warning) alert
Hazard level 4 = Warning alert

In case of equal hazard levels, aural priority was given to reactive system alerts above forward-looking system alerts. To suit special intentions of FM(AG07), "Advisory" and "Caution" alerts were both given in a performance *decreasing* windshear situation. Normally, Flight deck Alerting Systems, if related to windshear systems,[9, 25] define "Caution" alerts for performance *increasing* shears. Table 5 presents the aural and visual alerts used in the 1994 experiment.

Rouwhorst & Haverdings

Threat-level determination

With the reactive system the threat-level was determined by comparing the averaged F-factor, computed through Eq.(3) and Eq.(4), with critical limits defined.

Using the forward-looking windshear detector, the threat level was determined, in real time, by an along beam averaged F-factor, calculated from a regression formula given by:

$$F_{L,av} = 14.922 * (\frac{\Delta V_D}{\Delta r}) + 0.005 \qquad (17)$$

This regression formula, established by a model fit to radar-determined data of actual microbursts[24], uses the peak-to-peak speed difference (ΔV_D) divided by the distance between the peaks (Δr).

In the regression analysis a sine wave model was used for a spatial approximation of the windshear effect over a length of one kilometre, including a vertical wind component estimation. The model assumes that all performance-decreasing shear occurs between the velocity peaks of the sine wave. It was found for almost all microbursts that Δr varied between 2 and 6.2 km, and the fit obtained showed a correlation coefficient of 0.999 [24].

For every scan cycle and for every windshear cell (vortex), the laser model determined the value(s) of ΔV_D along the laser beam and the corresponding Δr according to:

$$\Delta V_D = V_{Doppler(max)} - V_{Doppler(min)} \qquad (18)$$

The radius of the icon would be given by:

$$r_{icon} = \frac{| R_{V_{Doppler(max)}} - R_{V_{Doppler(min)}} |}{2} \qquad (19)$$

using the along beam range points for the maximum and minimum Doppler speed derived. Finally, the calculated icon radius was used to determine Δr:

$$\Delta r = 2 * r_{icon} \qquad (20)$$

Per windshear cell, the one-kilometre averaged laser F-factor ($F_{L,av}$) was established and tested against critical F-factor levels to derive the hazard status, see Table 6.

It is noted that in the 1993 and 1994 experiments, both for the reactive and the laser system, the F-factor definitions were such that negative F-values implied a *decreasing* aircraft performance.

Table 5 Aural alerts and EFIS/PFD labels per system as function of the hazard status

Hazard Status	Voice [2]	Label Colour	PFD label of Laser system	PFD label of Reactive system
0	---	none	---	---
1	"ADVICE..."	blue	WINDSHEAR AHEAD	WINDSHEAR
2	"CAUTION..."	amber	WINDSHEAR AHEAD	WINDSHEAR
3 [1]	"CAUTION..."	amber & red	WINDSHEAR AHEAD	---
4	"WARNING..."	red	WINDSHEAR AHEAD	WINDSHEAR

Notes: 1) Only used in case of a display, in order to suppress Warning alerts until icon moves from zone B into zone A.

2) Aural messages following "ADVICE...", "CAUTION..." or "WARNING..." are identical to PFD text labels in 4th and 5th column and were announced in two subsequent cycles.

Table 6 Hazard levels as function of critical F-factors

level	Critical F-factor
0	> -.040
1	between -.040 and -.100
2	between -.100 and -.210
3	< -.210
4	< -.210

EFIS/NAV-display presented windshear icons

When the scanning mode of the laser/lidar detected a windshear ahead of the aircraft, a windshear icon would be presented on the EFIS/NAV display. Sometimes multiple windshear cells were used, then multiple icons could occur, see Fig.29. Icons indicated the relative threat (hazard) of the windshear to the aircraft by their position, size and colour. The nearer the icon is to the intended flight path, the greater the windshear hazard on the aircraft and perceived threat by the pilot. Alert zones were defined to incorporate this effect.

Windshear icon display alert zones

Based on information from a NASA/Industry proposed concept[25,26], the following icon alert zones were defined, see Fig.28. Zone A is given by the region bounded by an arc with a radius of 1667 m (0.9 nm) and with a maximum azimuth angle of ± 25 degrees, and two vertical lines, having 463 m (0.25 nm) lateral displacement on either side of the aircraft's longitudinal axis. Zone B is defined by a plane with a radius that

related to the 4 nm maximum detection range of the laser (or about 8 km) and with a maximum azimuth angle of ±45 degrees relative to the same longitudinal axis. Zone B excluded sector A.

If one or more icons were infringing alerting zone B or A, then the icon with the highest threat-level determined would trigger the FAS. To prevent too many unnecessary go-arounds from being initiated while still having time to undertake action, any 'warning' hazard outside sector A would be presented to the crew in the form of combined amber/red circles (implying a hazard level 3). In this way it was made clear to the crew that the windshear already possessed the most severe threat to the aircraft, but that there was still time to monitor the icon (dynamics) on the display, to assess circumstances and to negotiate about possibilities to solve the safety endangering situation. However, the moment a (still) amber/red icon moved into alert sector A, it would be coloured fully red and the FAS would revert to hazard level 4, producing an aural warning alert, see Tables 5 and 7. Any warning (red) alert implied a direct go-around initiation.

EFIS/PFD presented windshear labels

Whenever a windshear sensor detected a windshear of a certain hazard level, windshear labels were presented on the EFIS/PFD, see Fig.30 and Tables 5 and 6. It was assumed that this would give the pilot flying better awareness about the sensor that actually detected the windshear. Based on pilot comments from the 1993 experiment, the windshear label positions were reversed: reactive labels on the top of the PFD and forward-looking windshear labels on the bottom side of the PFD. An example of EFIS/NAV-presented windshear icons and the corresponding windshear labels on the PFD can be found in Figures 29. There three lidar-detected windshear cells (icons) are shown on the NAV-display

Rouwhorst & Haverdings

Table 7 EFIS/NAV presented windshear icon colours and laser hazard status

Hazard Status	Icons in or infringing	
	Zone A	Zone B
0	-	-
1	BLUE	BLUE
2	AMBER	AMBER
3	-	AMBER & RED
4	RED	RED

(respectively coloured as red, amber and amber/red from bottom to top), of which the highest threat-level is given by a red icon very near to the aircraft. A red alert label presented on the lower part of the PFD corresponds to this threat-level. Simultaneously, the reactive system also shows the presence of a windshear, as indicated by the amber (caution) label.

Speed increment procedure

A speed increment flight procedure was set up and evaluated based on the 'cautious' penetrating windshear flight procedure that came out best from the 1993 experiment. Altitude dependency was left out. Pilots did not have to interpret the alerts themselves anymore, since the procedure developed was coupled to the integrated, threat-level based, alerting concept. Whenever an aural alert was passed on to the cockpit, the pilot either applied a speed increment and continued the approach, or initiated a go-around in case of *any* red, i.e. level 4, alert. The speed additives belonging to hazard level 1, 2 or 3, were respectively 5, 15 or 20 kts, with respect to $V_{FAS}=155$ kts ($= V_{ref}+$ 5 kts).
Although human auditive memory is relatively long, a visual reminder was found necessary. Therefore, a blue flashing (lying V) symbol would appear on the speed tape (left side of the PFD) whenever a new speed setting was advised, to be set in the auto throttle window, see Fig 30. Lowering the (AT-window) speed would not be indicated, but was left free to the crews.

Windshear icon display concept

Two different concepts of windshear icon displays were evaluated. The first concept (display A) displayed icons that were "static" in nature. "Static" here means that the icon colour would only vary as the windshear threat-level would change to a different level, but that colours would remain the same despite the speed increment(s) applied by the pilot. In the second concept (display B) the icon colours were adapted when an AT-speed increment was applied, through modification of the alert (and colour) thresholds. Crews would thus have a

visual feedback of speed actions enabling them to see if a reduction of the relative windshear threat had taken place. This concept will be referred to as *speed feedback*. It was expected that this visual feedback presented by display B would improve the overall situational awareness and thereby crew (pilot) decisions and that the number of go-arounds would be reduced.

Experimental factors

Some of the factors that were varied in the experiment, and that will be briefly addressed below, were:

1) Look-ahead distance (0m / 1600m / 2400m)
2) Display type (no icon display/ display A/ display B)
3) Downburst strength (not extreme/ extreme)
4) Downburst threat position (no threat/ threat)

Preliminary results

So far, only a few initial results of crew workload can be shown. Workload was derived using the McDonnell [23] "demand on the pilot" interval scale. The individual ratings from both the pilot flying and the PNF were combined into a total crew score.
When analyzing runs *without* a windshear icon display (sub-experiment 1), it turned out that downburst strength had a statistically significant effect on crew workload $(F(2,40)=3.30; p<0.0471)$, see Fig.31. Especially for the extreme downburst severity, if no look-ahead sensor was available, crew workload was much higher than for the not extreme cases. For the latter, crew workload remained almost constant when adding a look-ahead sensor, since differences shown are statistically insignificant $(F(2,40)=0.203; p<0.8172)$. For the extreme cases crew workload reduced significantly $(F(2,40)=4.78; p<0.0138)$ with more forward-look range.
First results from the second sub-experiment showed that adding the windshear icons to the NAV-display reduced crew workload significantly, see Fig.32. The reduction was almost totally due to the reduction in workload of the PF, since workload of the PNF remained the same, because of a much improved situational awareness.
On the other hand, the application of the speed feedback mechanism increased crew workload. The speed feedback mechanisme 'forced' the crew to continue the approach towards/into the shear. Especially with a display the interpretation of the varying colour of an icon as a result of the speed feedback concept caused an additional increase in mental workload.
Fig. 33 presents results for downburst strengths categorized into 'extreme' and 'not extreme' cases. In the latter case crew workload reduced for icon display type A, but increased for display type B. For the extreme windshear cases (implying a crash would almost certainly occur, if flown through) adding display type A

Rouwhorst & Haverdings

1843

hardly changed crew workload, but it significantly decreased for display type B. Regardless of this, display type A scored a lower (.e. better) crew workload.

Icon position ('no threat' or 'threat') was statistically not significant, but the interaction with 'displays' and 'speed feedback' was $(F(1,40)=21.07; p<0.0000)$. Results indicated a significant reduction (from 5.6 to 4.6) in crew workload for display A for the no threat cases. For the threatening icon positions, no significant differences in workload were found between both types of displays.

Based on an analysis of questionnaire data from every run, pilots preferred display type B above type A. Nevertheless, from the debriefing results a minor (statistically non-significant) preference for display type A was found, see Fig.34. The reason for this was that display B tended to drive them to continue the approach towards a worsening (less safe and workload increasing) windshear situation. Since they regarded a severe windshear as a once-in-a-lifetime experience, they would not object to make a go-around.

Some pilot comments

From pilots comments it was learned that the windshear icon display concept and the integrated aural alerting mechanism were liked very well. However, the hazard level 1 alert (and the 5 kts speed increment that had to be applied) was not found useful and therefore should be left out totally in the future. Presenting level 1 (blue) icons on the NAV-display was found acceptable.

One crew disliked the use of the PFD label "WINDSHEAR" in a situation where the flight would be continued with an increased speed. It should be reserved for the moment that immediate windshear awareness/action is required.

According to most crews, the windshear icons improved situational awareness and contributed positively to an earlier decision making. Nevertheless icon sizes and colours changed too frequently and a more stable presentation was desired.

Related to handling issues, most pilots commented they missed the possibility to perform (laser) tilt control, like that of a weather radar.

Pilot opinions were not unanimous on the speed feed back concept and the usefulness of the (flashing) speed increment advisory symbol on the PFD speed tape. More comments on these (and other) issues involved will be published in the future.

Concluding remarks

Conclusions given should be regarded as preliminary. It can be concluded that presentation of windshear icon information, derived from forward-looking laser/lidar sensors on the map-mode of an EFIS/NAV-display, is a very feasible concept. Icons improve the awareness of the windshear situation during the approach and reduces

crew workload significantly. This beneficial effect was relatively stronger for display concept A (no speed feedback) than for display concept B (with speed feedback). The speed feedback mechanism increased crew workload, regardless of the presence of a display.

When implementing a forward-looking windshear detection system in conjunction with a reactive system, a threat-level based *aural* alerting should be applied. Seen in the context that one should strive for the minimum necessary (extra) cockpit alerts, it can be concluded that the hazard level 1 aural cues tested can be left out. However, displaying blue (hazard level 1) icons may be allowed. The sensor-based alert label presentation on the EFIS/PFD was well received by the pilots, since awareness about which sensor provided an alert was found very important.

References

1. *"Forward-looking windshear radar"*, Flight International, page 42, 14-20 February 1996.
2. Frederick, G., *"Forward-looking windshear radar"*, paper presented at the World Aerospace Technology International'95 conference.
3. *"Windshear teamings for US business"*, Flight International, page 8, 24-30 August 1994.
4. Anon. FAA: Windshear Training Aid, Example Windshear Training Program, February 1987.
5. FAR, Code of Federal Regulations, Parts 60 to 139, Revised as of January 1, 1995.
6. *"Collins windshear radar approved"*, Flight International, 26 July-1 August 1995, page 21.
7. *"Westinghouse Electric received supplemental type certification"*, Avionics Magazine, January 1996, page 16.
8. *"Westinghouse's windshear radar gains approval"*, Flight International, 22-28 November 1995.
9. *"Flight Deck Alerting System (FAS)"*, Aerospace Recommended Practice, ARP 4102/4, July 1988.
10. Haverdings, H.; Rouwhorst, W.F.J.A., *"Initial results of a piloted simulator investigation of modern windshear detection systems"*, ICAS-paper 7-1., ICAS 1994 Conference, Anaheim, Sept. 1994.
11. Swolinksy, M., *"Windshear models for aircraft hazard investigation"*, AGARD Conference Proceedings, CP-470, May 1989.

Rouwhorst & Haverdings

12. Schultz, T.A., *"Multiple Vortex-ring Model of the DFW Microburst"*, Journal of Aircraft, Vol.27, No.2, February 1990.
13. Wingrove, R.C.; Bach, R.E.,*"Severe winds in the DFW microburst measured from two aircraft"*, AIAA paper 87-2340-CP, Aug.1987.
14. Jansen, C.J., *"Non-Gaussian Atmospheric Turbulence Model for Flight Simulator Research"*, paper AIAA 80-2568R 7th Atmospheric Flight Mechanics Conference, Danvers, August 1980.
15. Woodfield, A.A.; Woods, J.F., *"Worldwide experience of windshear during 1981-1982."* AGARD Conf. on Flight Mechanics and System Design Lessons from Operational Experience, AGARD-CP-347, May 1983.
16. Glover, H., *"Windshear Detection and Recovery Guidance: an Equipment Manufacturer's Perspective"*, Sundstrand Data Control Inc., Proceedings of the Windshear One Day Conference of the Royal Aeronautical Society, 1 November 1990, London.
17. Bowles, R.L., *"Reducing Windshear Risk Through Airborne Systems Technology"*, 17th Congress of the ICAS, Sweden, 1990.
18. Anon. FAA Technical Standard Order *"Airborne Windshear Warning and Escape Guidance for Transport Airplanes"*, FAA TSO-C117,24-07-1990.
19. Anon. FAA Advisory Circular *"Criteria for Operational Approval of Airborne Wind Shear Alerting and Flight Guidance Systems"*, FAA-AC-120-41, 11/7/1983.
20. *"Joint Airworthiness Requirements JAR-AWO All Weather Operations"*, Change 1, effective 29 November 1985, Joint Airworthiness Authorities.
21. Zijlstra, F.R.H.; van Doorn, L.,*"The construction of a subjective Effort Scale"*, Report Technical University Delft, Department of Social Sciences & Philosophy, 1985.
22. Siegel, S.; Castellan Jr.,N.J., *"Nonparametric statistics for the behavioral sciences"*, 2nd intern. edition, McGraw-Hill Book Company, 1988.
23. McDonnell, J.D.,*"Pilot rating techniques for the estimation and evaluation of handling qualities"*, AFFDL-TR-68-76, December 1968.
24. Elmore,K.L.; Sand, W.R., *"A cursory study of f-factor applied to Doppler radar"*, paper 3rd Intern. Conf. on Aviation Weather Systems, Jan-Feb 1989.
25. *"Airborne Windshear Systems"*, Aerospace Recommended Practice, ARP 4102/11, Rev.B, 29-06-1993.
26. Hinton, D.A.; Osequera, R.M., *"Microburst avoidance crew procedures for forward-look sensor equipped aircraft"*, paper AIAA-93-3942, AIAA, Aircraft Design, Systems and Operations Meeting, Monterey, CA, August 1993.

Rouwhorst & Haverdings

APPENDIX A: Probability calculations

List of symbols

Erf	Error function
i	index
n_k	number of variables on segment k
Q	value of error function
SR_k	Safety Risk on k^{th} segment
TSR	Total Safety Risk per run
x	normal variable
y	limit value of normal variable
α	normalized upper boundary value for risk exceedance
β	normalized lower boundary value for risk exceedance
ϵ	higher order error term
μ	mean value of normal variate
σ	standard deviation of normal variate

A.1 General probability calculations

When calculating the probability of $x_i > \alpha_i$, where x_i is a normal variate, then this probability equals $Q_i(\alpha_i)$, where

$$Q_i(\alpha_i) = \text{Prob}(x_i > \alpha_i) \qquad (A.1)$$

where use is made of the error function 'Erf', which is based on the normal distribution.

$$Q_i(\alpha_i) = \text{Erf}(x_i > \alpha_i) \qquad (A.2)$$

so that $Q_i(\alpha_i)$ can be calculated applying a standard method, see Abramowitz and Stegun (1964) [A.1].
Because of the symmetric distribution we also have:

$$\text{Erf}(x_i < -\alpha_i) = \text{Erf}(x_i > \alpha_i) \qquad (A.3)$$

or:

$$\text{Erf}(x_i > -\alpha_i) = 1 - \text{Erf}(x_i < -\alpha_i)$$
$$= 1 - \text{Erf}(x_i > \alpha_i) \qquad (A.4)$$

so that:

$$\text{Erf}(x_i > -\alpha_i) = 1 - Q_i(\alpha_i) \qquad (A.5)$$

or, in combination with Eq.(A.1):

$$Q_i(-\alpha_i) = 1 - Q_i(\alpha_i) \qquad (A.6)$$

In case of a double-sided probability of the form:
$$\text{Prob}(\beta_i < x_i < \alpha_i) \qquad (A.7)$$
the probability is split up in two parts, viz.:
$$\text{Prob}(\beta_i < x_i < \alpha_i) = \text{Prob}(x_i < \alpha_i) + \text{Prob}(x_i > \beta i) \quad (A.8)$$

For example, the touchdown distance should not be less than -1000' or not be more than 3800', then this double-sided probability is split up in two probabilities, viz.:
1. probability that $x < -1000'$, or
2. probability that $x > +3800'$.
To each of these probabilities the same methodology is applied.

For each variate x_i involved in the flight or landing probability the error function is applied.
The safety risk 'SR_k' on the kth segment (segment 1"upper ILS", segment 2 "lower ILS", segment 3 "go-around", segment 4 "landing") is the composite of all the contributions $Q_i = Q_i(\alpha_i)$, according to Eq.(10a) of the main text, applied repeatedly:

$$SR_k = \sum_{i=1}^{n_k} \{Q_i\} - \sum_{i=1}^{n_k-1} \{Q_i \cdot \sum_{j=i+1}^{n_k} Q_j\} + \varepsilon \qquad (A.9)$$

where n_k denotes the number of variates per segment.
Since the higher error term ε is very small this term has been deleted from the calculations.
A table of variates per segment is given in Table A.1.

The total safety risk, 'TSR', per run is then calculated by summing the safety risk contributions from those segments which are involved in either the landing approaches or the go-around approaches, i.e.:

$$TSR = \sum_{k=1,3} SR_k \quad \text{for go-arounds on 1}^{st} \text{ segment}$$

$$(A.10.a)$$

or

$$TSR = \sum_{k=1,2,3} SR_k \quad \text{for go-arounds on 2}^{nd} \text{ segment}$$

$$(A.10.b)$$

or

$$TSR = \sum_{k=1,2,4} SR_k \quad \text{for landing approaches} \quad (A.10.c)$$

A.2 Safety risk
In order to calculate the probability of a variable to exceed some limit value $y_i(k)$ the function $Q_i(\alpha_i(k))$ is used.
The normalized limit value $\alpha_i(k)$ is calculated from the limit value $y_i(k)$ for the kth segment using the mean $\mu_i(k)$ and standard deviation $\sigma_i(k)$ of the ith variable under question as follows:

$$\alpha_i(k) = \frac{[y_i(k) - \mu_i(k)]}{\sigma_i(k)} \qquad (A.11)$$

Here $\alpha_i(k)$ has a mean of zero and standard deviation of 1.
Values for $y_i(k)$ are given in Table A.1 for the flight segments and for the landing segment.
The values of $\mu_i(k)$ and $\sigma_i(k)$ were determined by the post-processed segment statistics for the x_i-th variable.

Table A.1 Variables per segment for risk calculation

x_i	SEGMENT [1]			
	1	2	3	4
α_{margin}	0	0	0	0
$V_{a\,max}$	190 kts	190 kts	238 kts	-
$A_{z\,max}$	+2.5 g	+2.5 g	+2.5 g	-
$A_{z\,min}$	-0.5 g	-0.5 g	-0.5 g	-
$\Delta\epsilon_{G.P.}$	-2.0 dot	-2.0 dot	-	-
x_{TDmax}	-	-	-	3800 ft
x_{TDmin}	-	-	-	-1000 ft
y_{TDmax}	-	-	-	+21 m
y_{TDmin}	-	-	-	-21 m
$w_{c\,TD}$	-	-	-	1000 [2] ft/min
V_{GSmax}	-	-	-	203 kts
φ_{TDmax}	-	-	-	8.5 deg
φ_{TDmin}	-	-	-	-8.5 deg
θ_{TDmax}	-	-	-	11 deg

Notes: 1) For segment definition, see page 6.

2) 600 ft/min in case of $\theta_{TD} < 0$ deg.

A.3 References
A.1. Abramowitz, Stegun: "*Handbook of mathematical functions*". National Bureau of Standards, 1964.

Rouwhorst & Haverdings
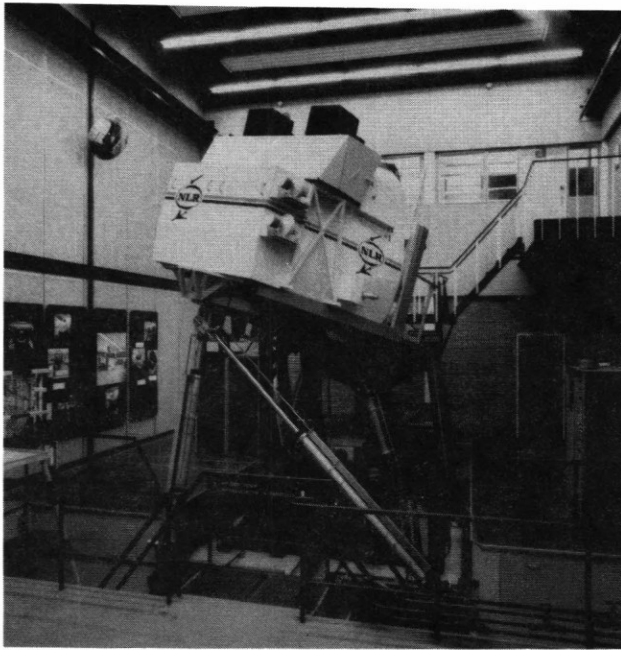
Fig.1 NLR's four degrees-of-freedom
Research Flight Simulator

Fig.3 Distribution of number of go-arounds

Fig.2 Research Flight Simulator Cockpit
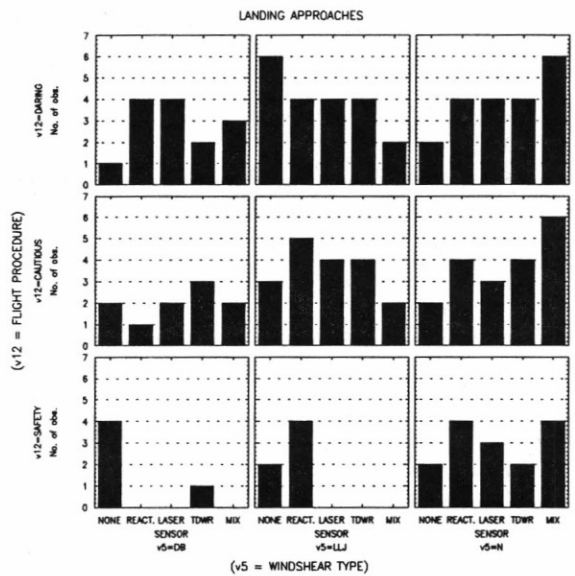
Fig.4 Distribution of number of landing
approaches

Rouwhorst & Haverdings

1847

DISTRIBUTION OF NUMBER OF GO AROUNDS ALONG THE ILS AND NUMBER OF LANDINGS
(N=180; measurement runs of all crews)

Fig.5 *Distribution of number of go-arounds and landings*

T-test: t= 3.922; p= .000; n1+n2= 18+33
N. of Cases = 51
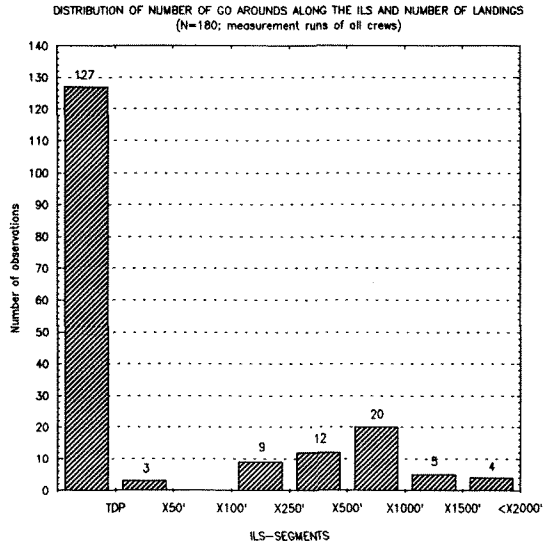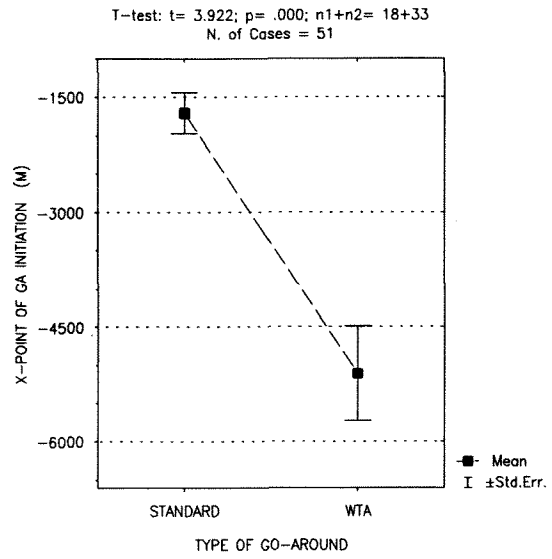
Fig.7 *Distribution of go-around type over distance of go-around initiation relative to the TDP.*

FLIGHT PROCEDURE main effect
$F_{(2,29)}=4.23$; $p<.0244$
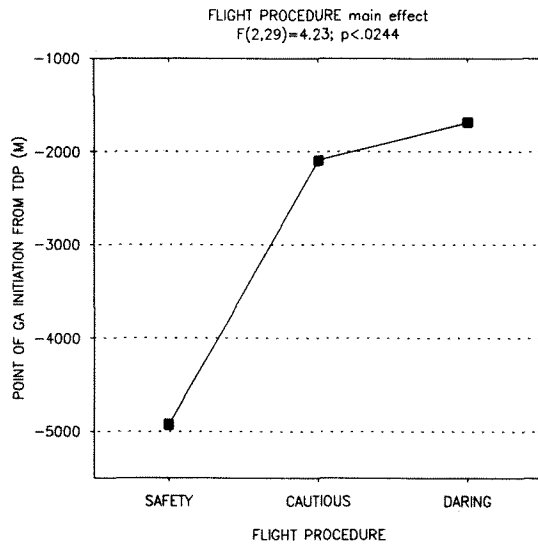
Fig.6 *Effect of flight procedure on moment of go-around initiation relative to the TDP*

Kruskal-Wallis test: H(2, N= 52) = 9.4899   p =.0087
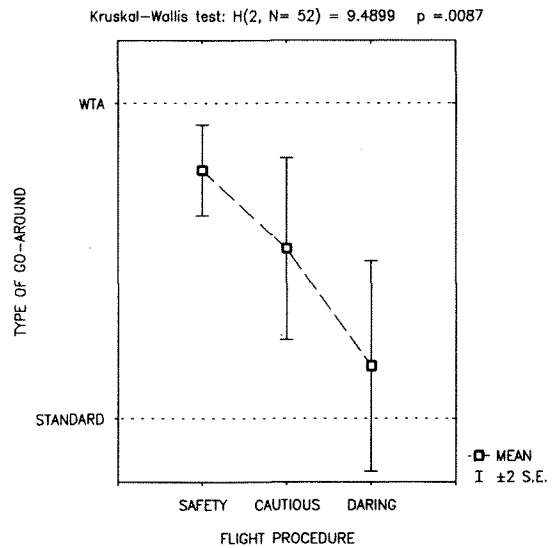
Fig.8 *Effect of flight procedure on type of go-around*

Rouwhorst & Haverdings

1848
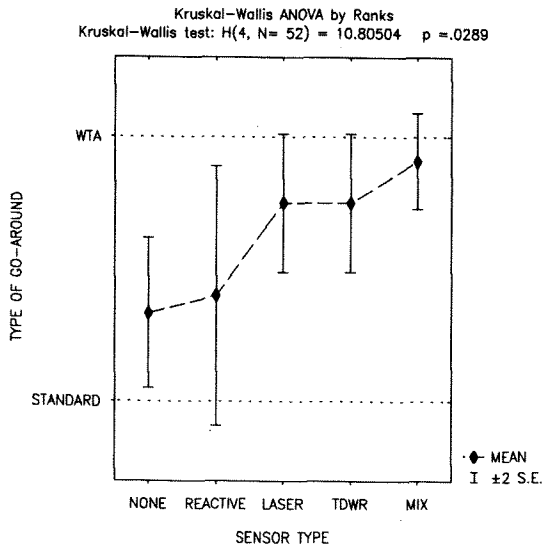
Fig.9 *Effect of sensors on type of go-around*
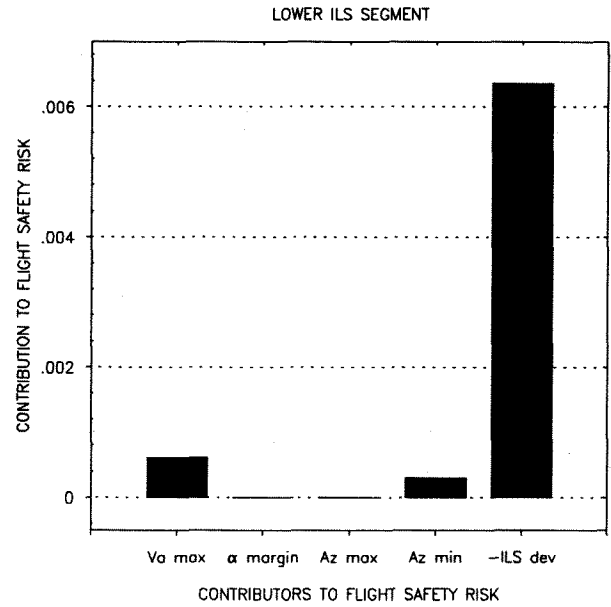
Fig.11 *Contributors to flight safety risk*
- lower ILS segment
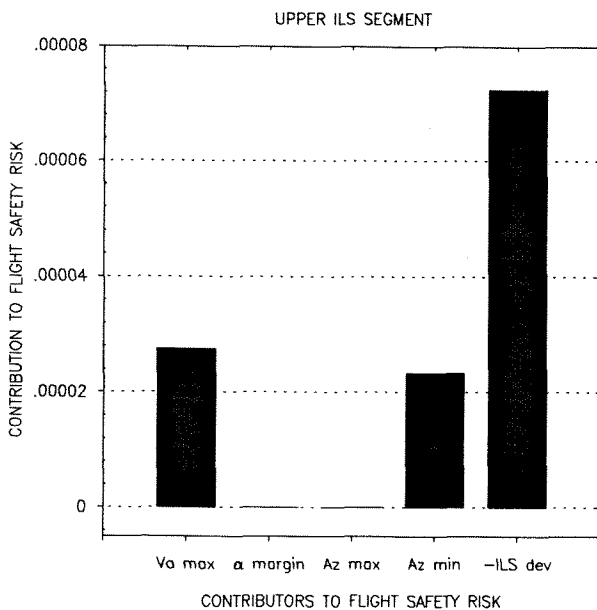
Fig.10 *Contributors to flight safety risk*
- upper ILS segment
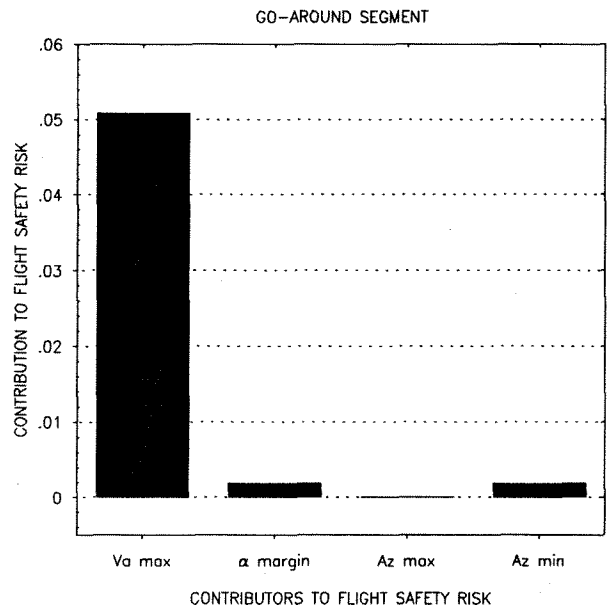
Fig.12 *Contributors to flight safety risk*
- go-around segment

Rouwhorst & Haverdings
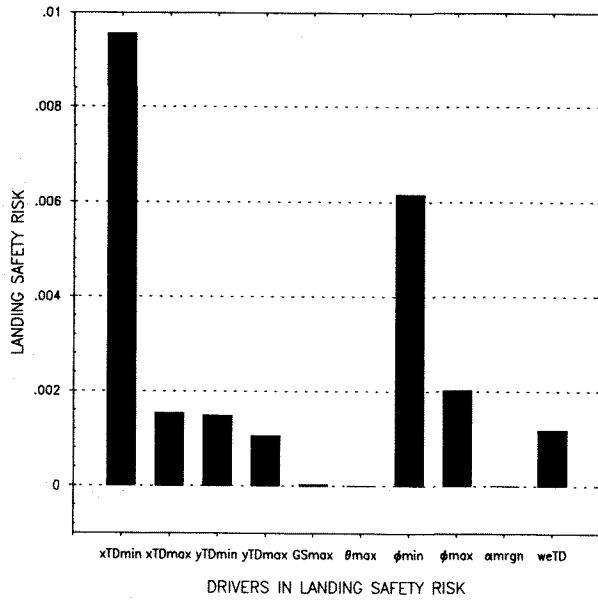
Fig.13 Contributors to landing safety risk
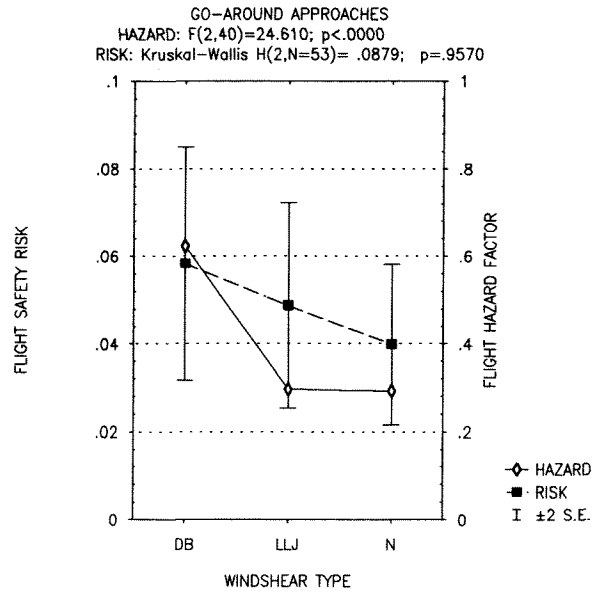
Fig.14b Effect of windshear on flight safety during go-around approaches
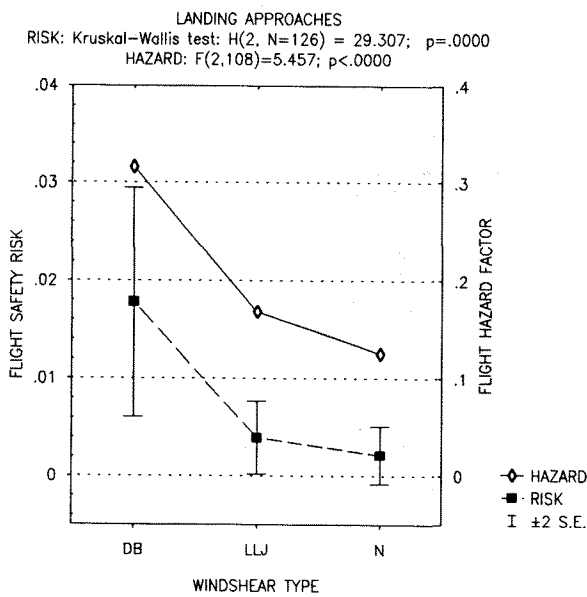
Fig.14a Effect of windshear on flight safety during landing approaches
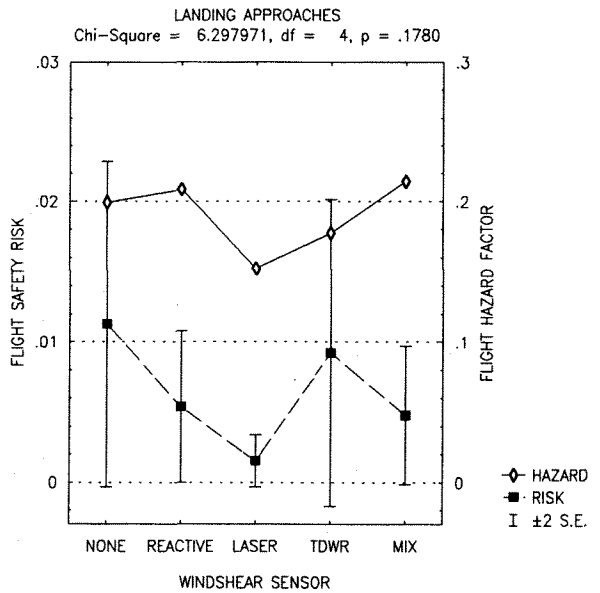
Fig.15 Effect of windshear sensors on flight safety for landing approaches

Rouwhorst & Haverdings
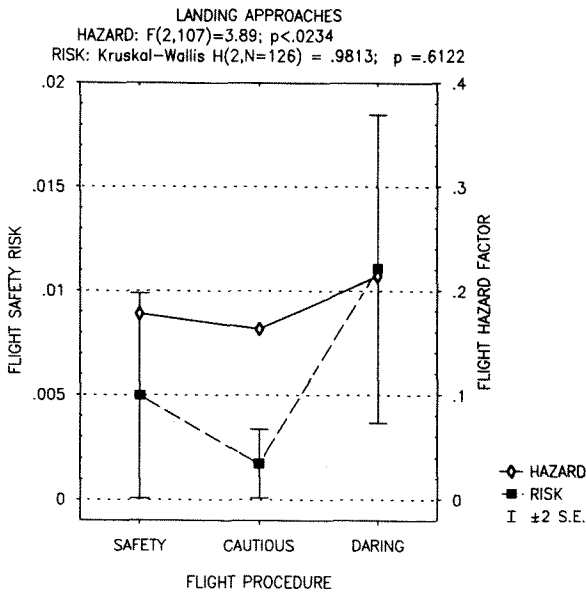
Fig. 16a Effect of flight procedure on flight safety for landing approaches
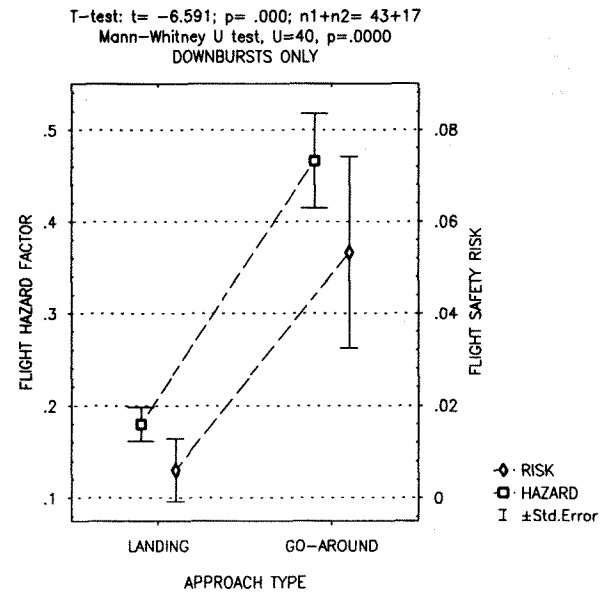
Fig. 17 Effect of approach type on flight safety risk and hazard factor
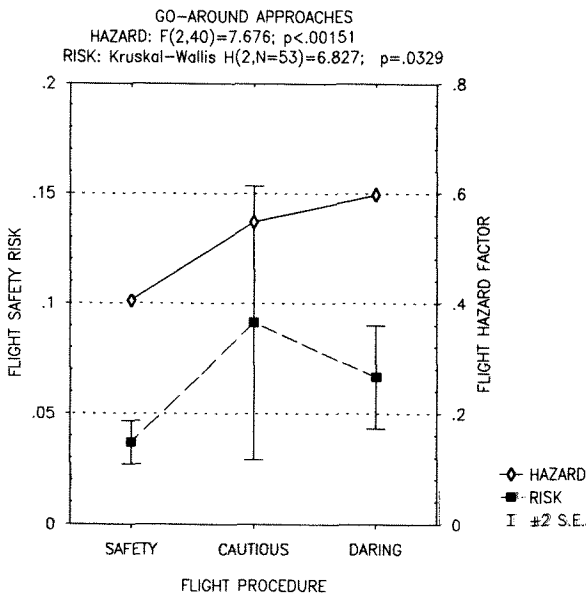
Fig. 16b Effect of flight procedure on flight safety for go-around approaches
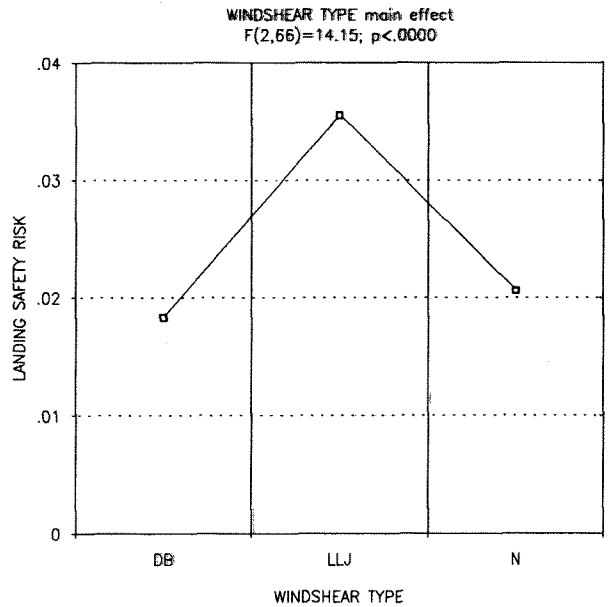
Fig. 18 Effect of windshear type on landing safety risk

Rouwhorst & Haverdings

FLIGHT PROCEDURE main effect
F(2,66)=11.53; p<.0001
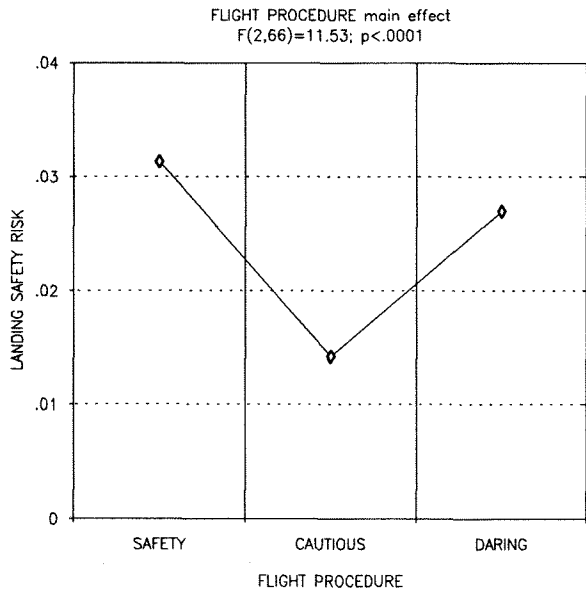
Fig.19 Effect of flight procedure on landing safety risk

WINDSHEAR SENSOR main effect
F(4,66)=7.45; p<.0001
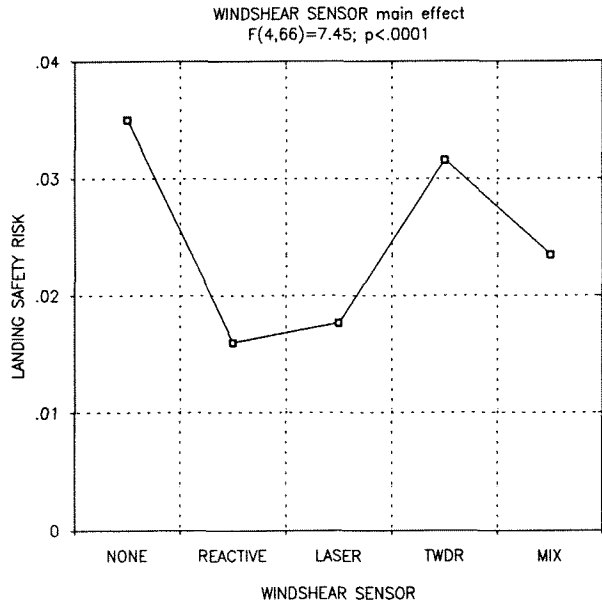
Fig.21 Effect of windshear sensor on landing safety risk
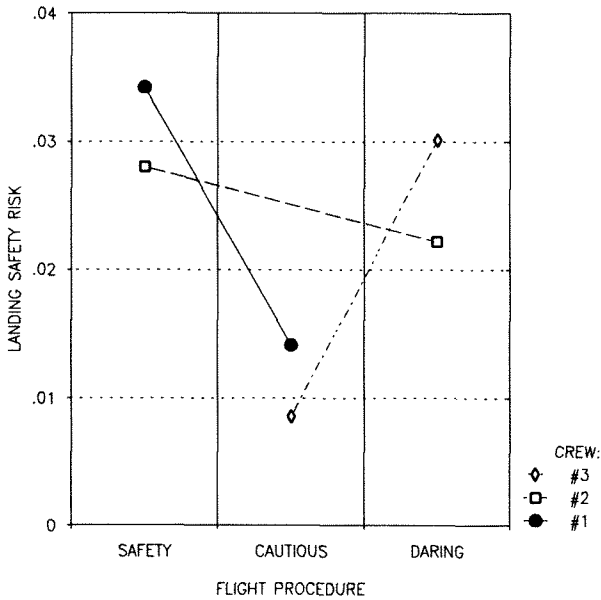
Fig.20 Effect of crews, nested within flight procedures, on landing safety risk

WINDSHEAR TYPE main effect
F(2,104)=2.91; p<.0587
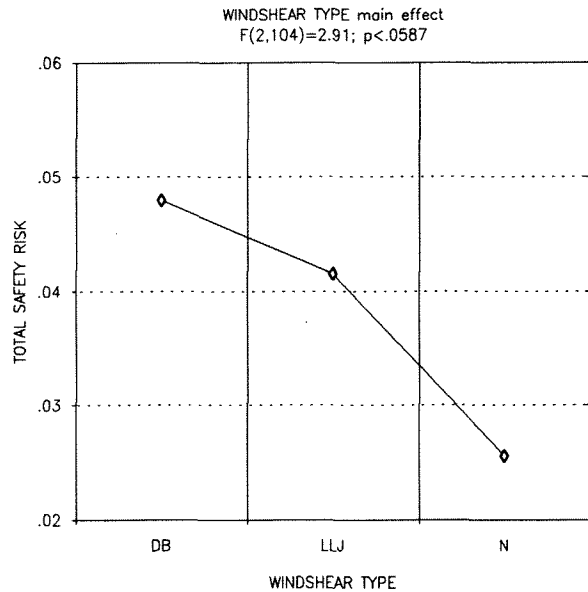
Fig.22 Effect of windshear type on total safety risk

Rouwhorst & Haverdings
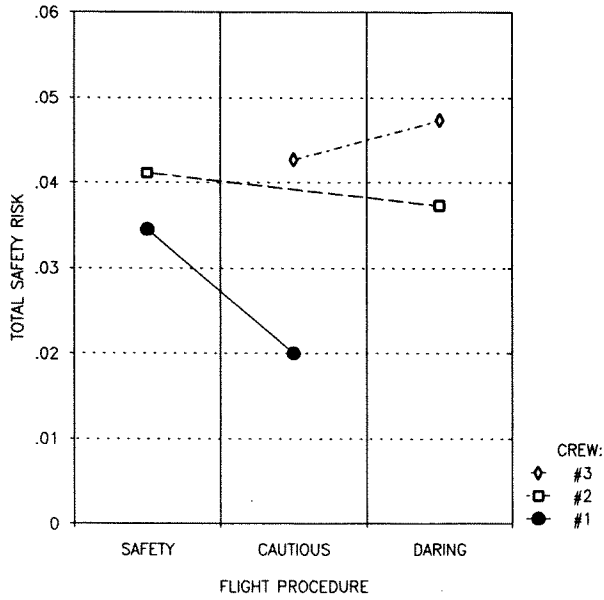
Fig.23 *Effect of crews on total safety risk*

FLIGHT PROCEDURE main effect
Go-arounds: $F_{(2,19)}=2.35$; $p<.1220$
Landings: $F_{(2,69)}=11.14$; $p<.0001$
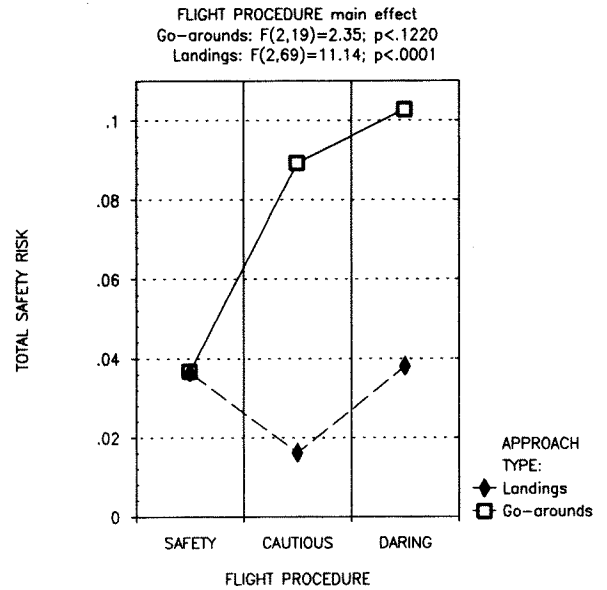
Fig.25 *Effect of flight procedure on total safety risk*

WINDSHEAR SENSOR main effect
$F_{(4,104)}=1.92$; $p<.1123$
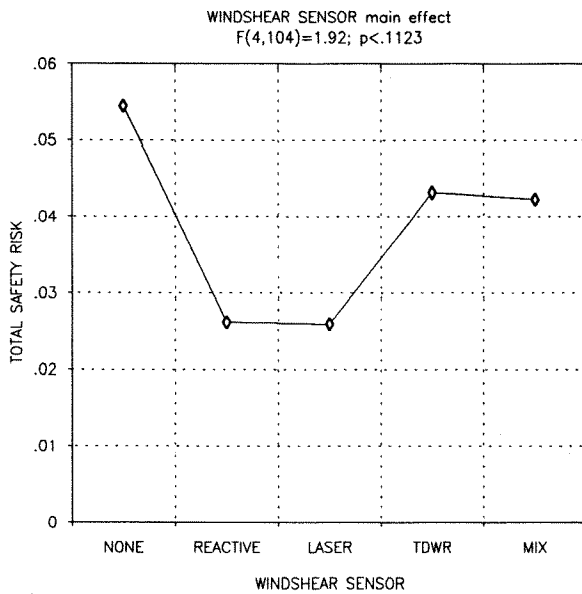
Fig.24 *Effect of windshear sensors on total safety risk*

APPROACH TYPE main effect
TOTAL SAFETY RISK: $F_{(1,117)}=17.69$; $p,.0001$
FLIGHT SAFETY RISK: $F_{(1,117)}=59.62$; $p<.0000$

Fig.26 *Effect of approach type on total safety risk*

Rouwhorst & Haverdings

1853

APPROACH TYPE main effect
TOTAL SAFETY RISK: $F_{(1,117)} = 12.24$; $p < .0007$
FLIGHT SAFETY RISK: $F_{(1,117)} = .3346$; $p < .564$
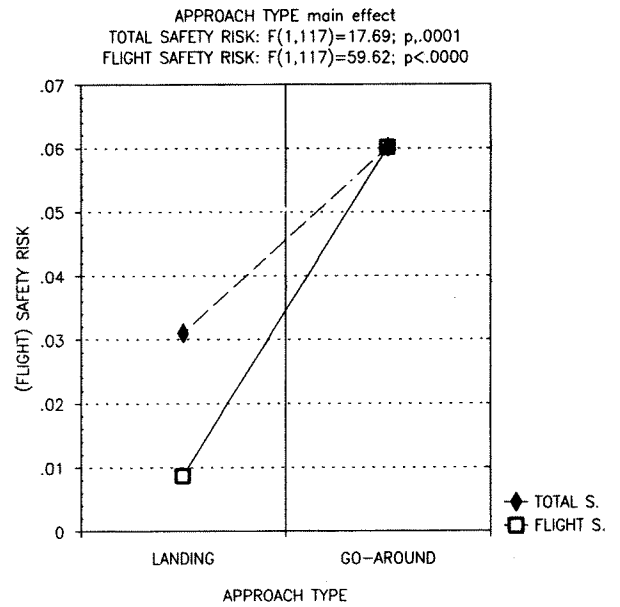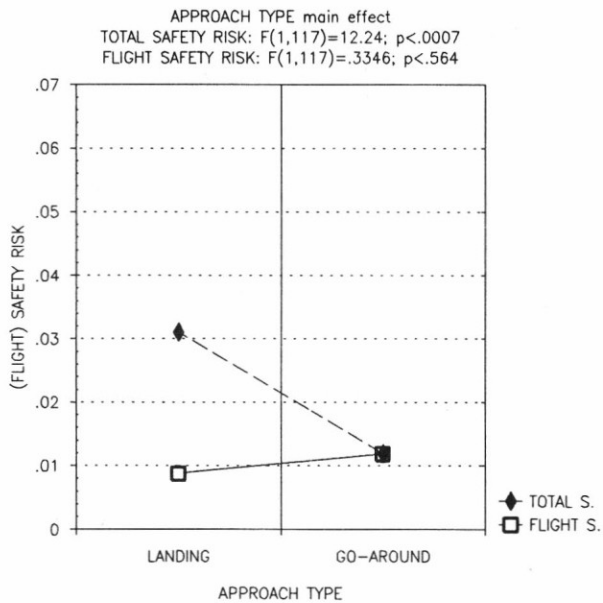
Fig.27 Effect of approach type on total safety risk; effect of airspeed in the go-around *excluded*
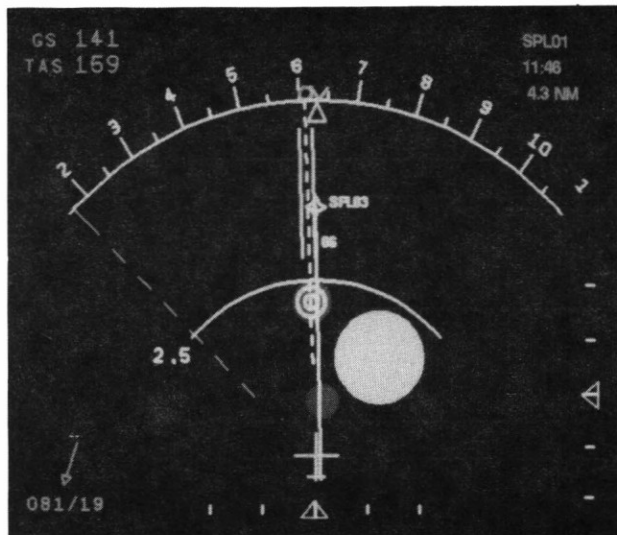
Fig.29 Navigation Display, showing three windshear icons (original shows colours Red, Amber and Amber/Red from bottom to top)
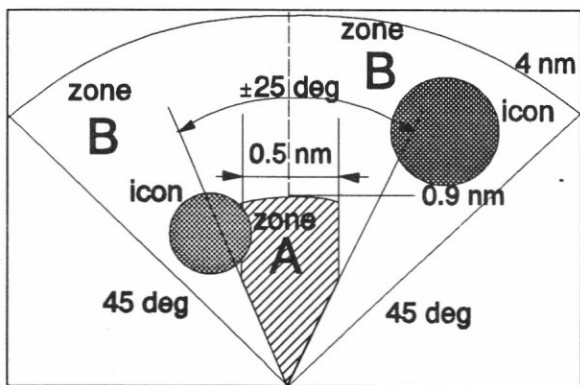

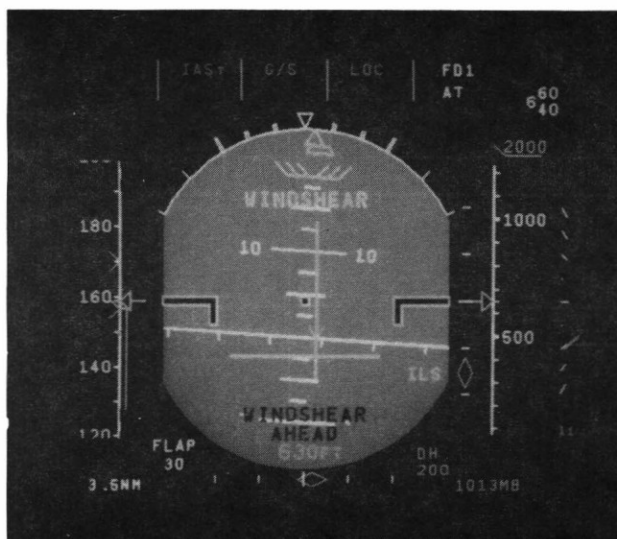Fig.28 Definition of hazard zones A and B

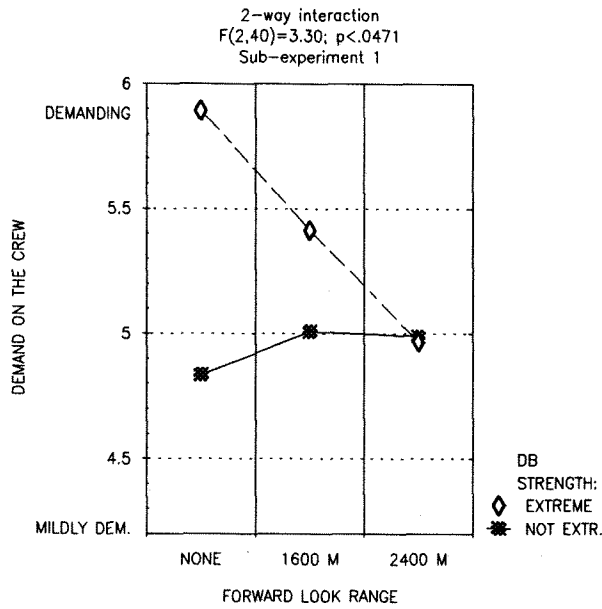Fig.30 Primary Flight Display, showing windshear alert labels and speed advisory symbol

Rouwhorst & Haverdings

2-way interaction
F(2,40)=3.30; p<.0471
Sub-experiment 1

Fig.31 Effect of forward-look distance on crew workload

3-way interaction
F(1,40)=14.32; p<.0005
Sub-experiment 2 (dry conditions)
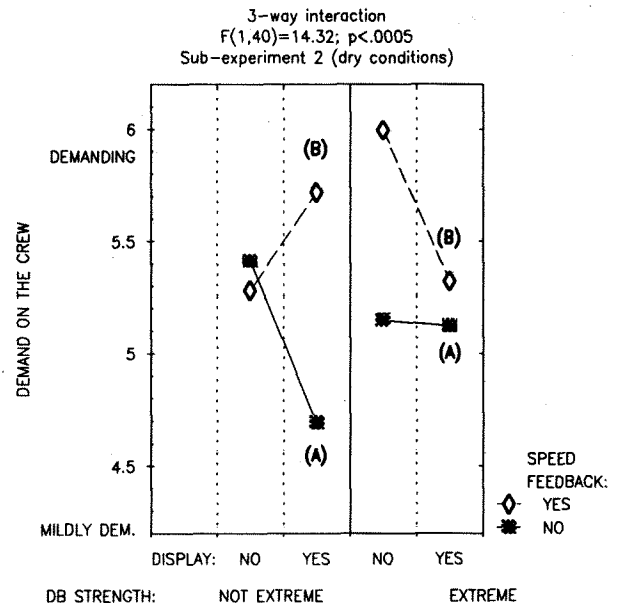
Fig.33 Effect of speed feedback and downburst strength on crew workload

2-way interaction
F(1,40)=1.12; p<.2972
Sub-experiment 2 (Dry conditions)
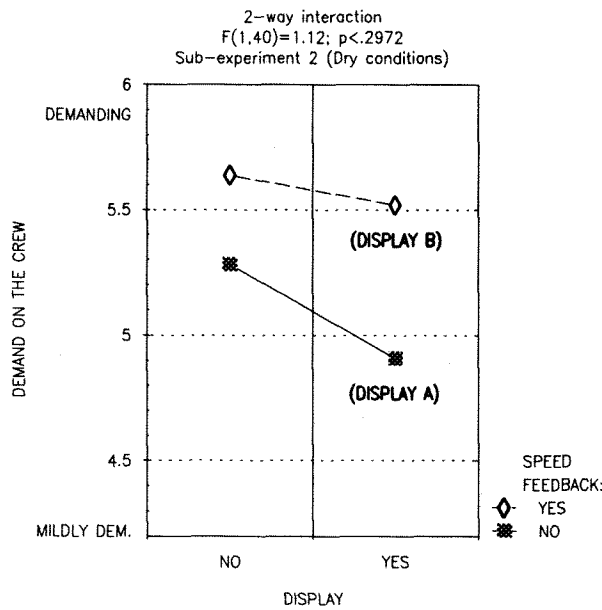
Fig.32 Effect of display and speed feedback on crew workload
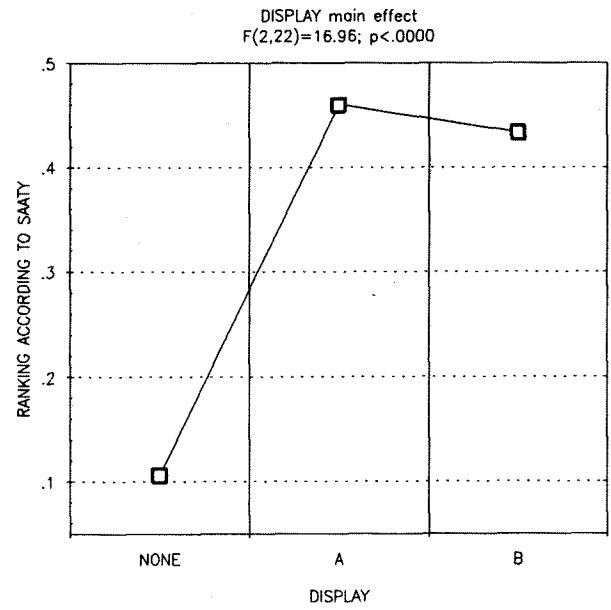

DISPLAY main effect
F(2,22)=16.96; p<.0000

Fig.34 Relative ranking of icon displays according to Saaty method

Rouwhorst & Haverdings

1855